3-27-2018

Vertical Sediment Accretion in Jamaica Bay Wetlands, New York

Ryan Christopher Clarke
Louisiana State University and Agricultural and Mechanical College

VERTICAL SEDIMENT ACCRETION IN JAMAICA BAY WETLANDS, NEW YORK

A Thesis

Submitted to the Graduate Faculty of the
Louisiana State University and
Agriculture and Mechanical College
in partial fulfillment of the
requirements for the degree of
Master of Science

in

The Department of Geology and Geophysics

by
Ryan Christopher Clarke
B.S., Louisiana State University and Agriculture and Mechanical College, 2016
May 2018

TABLE OF CONTENTS

ACKNOWLEDGEMENTS

I would like to thank Dr. Sam Bentley of the LSU Geology and Geophysics departments for his advising and guidance culminating in the research, implications and completion of this study. I would like to thank Dr. Hongqing Wang of the USGS for his aide and allowing us to use the USGS cores collected in Jamaica Bay. Dr. Carol Wilson for her help and extensive insight on New England marshes. Suyapa Gonzales, James Smith, and Brianna Crenshaw for their help in the processing stage of this study.

ABSTRACT

Over the last century, ~60% of the saltmarsh wetlands in Jamaica Bay (in the Gateway National Recreation Area of the Greater New York City region) have been converted to intertidal or subtidal unvegetated mudflats and projections suggest that all of Jamaica Bay's saltmarsh wetlands may disappear within the next two decades. After landfall of Hurricane Sandy in 2012 and to better understand environmental controls on the maintenance of the remaining Jamaica Bay wetlands, cores were collected from twelve saltmarsh locations in the bay to study the chronology of wetland vertical accretion and mineral sediment accumulation. In association with the United States Geological Survey Wetland and Aquatic Research Center (formerly National Wetlands Research Center), cores were analyzed for ^{137}Cs /^{210}Pb geochronology, percent mineral content, and total water content. Results show that averaged sediment accumulation rates for the wetlands are 0.48 cm-yr^{-1}. Analysis of sediment core mineral content indicates the uneven presence of a mineral-rich surface layer that is likely the result of sediment delivery from Hurricane Sandy. Results also document the presence of numerous subsurface layers of mineral-rich sediment interbedded between zones of organic-rich sediment. Based on various radionuclide chronologies, the estimated time of deposition, mineral-rich layers correspond to the known landfalls of major hurricanes near Jamaica Bay over the last nine decades. Collectively, these results suggest that sediments are delivered unevenly by landfalling hurricanes to coastal wetlands and that other phenomena that flood coastal wetlands with suspended sediments, such as extra-tropical storms, are important sediment sources as well.

INTRODUCTION

Coastal wetlands provide ecosystem services like flood protection, erosion control, water quality, and habitat for threatened and endangered species, but the land area within these wetlands is being reduced by subsidence and erosion of natural and anthropogenic causes (Pendleton, 2008). Many of these wetlands, such as ones found in southern Louisiana, have had significant land loss from the combined effects of subsidence (from underground fluid withdrawal and natural compaction), sea level rise, and lack of onland sediment distribution from levee construction (Blum and Roberts, 2009; Bentley et al., 2015). Recently with research looking at potential increases in hurricane frequency and intensity not only along the Gulf coast, but worldwide (Webster et al., 2005; Knutson et al., 2010; Holland et al., 2012) studies are beginning to quantify the impact these processes are having on our coasts (Smith et al., 2015). Hurricane Sandy brought this conversation to the New York region. Federal agencies such as the United States Army Corps of Engineers, National Park Service, the United States Geological Survey and state agencies such as the New York City Department of Parks & Recreation are now paying particular interest in Jamaica Bay with respect to its role as an important storm buffer (Wang et al., 2017).

Vertical mineral sediment accretion is important for the longevity of salt marshes (Turner et al., 2002). For long-term stability of tidal wetlands in an intertidal zone, the accumulation of mineral and organic matter must be in equilibrium or above sea level rising rates (Reed, 1990). Rate of increase of salt marsh platform elevation is limited by plant production, sediment supply, and subsurface processes (Chmura and Hung, 2004). The rate of wetland elevation change is representative of local accretion rates and erosion. In particular, discontinuous sediment deposition plays a necessary role in allowing many wetlands to stay above sea level. (Morris,

2016). Any changes to these controls can reduce vertical marsh accretion rates via a decrease in rate of deposition organic matter input, thus increasing rates of decomposition of inorganic sediment autocompaction (Reed, 1990).

Hurricane Sandy made its first United States landfall on Atlantic City, New Jersey on October 29, 2012, and carried Category 1 wind speeds into the New York City area that same day causing upwards of $19 billion in damages and an estimated $33 billion in restoration costs (Resilience, 2013). In Jamaica Bay, localized flooding proved to be an issue with flood levels reaching 5.4 meters during storm surge with the Federal Emergency Management Agency announcing the event as a "500-year coastal flood" (Orton et al., 2015).

New York is susceptible to flooding from nor'easters as well as hurricanes. Generated from the rapid deepening of an extratropical cyclonic low pressure area, nor'easters are storms that attack the New England area of the US in the winter. Initially a part of an extra-tropical storm traveling in the mid latitudes of the Atlantic Ocean, a nor'easter then breaks off usually due to bombogenesis (Hanafin et al., 2012). Nor'easters travel along the east coast causing coastal erosion and damage via winter precipitation and large wave action (Boustead, 2015). These systems attack the coast much more frequently than hurricanes, but generally have storm surges of a lesser magnitude (Karvetski et al., 2009; Siverd, 2013). One example is a 1992 storm reaching storm surge levels of 1.37 meters above predicted sea level at The Battery in New York, compared to Hurricane Sandy reaching 3.54 m above normal levels at the same location (Tanski, 2007).

Relative to the nor'easter in terms of structure, extratropical cyclones are low-pressure systems that have undergone extratropical transition driven by strong temperature gradients that exist in the atmosphere (Wang et al., 2013). In contrast, tropical cyclones, have little to no

temperature difference across the storm and are driven by a warm convection from the sea surface within the system (Jones et al., 2003). Structurally, the warm core in a tropical system is strongest near the earth's surface, while the extra tropical storm's "cold core" is in the troposphere. The transformation from a tropical to extra-tropical storm occurs most often when the cyclone's path will recurve to the northeast towards the United States; losing its strong core and circulation to a much more frontal featured system (Knutson et al., 2010).

Hurricanes are tropical cyclones developed in the Pacific or the Atlantic Ocean that reach wind speeds of 119 km/h. Beginning as a tropical disturbance, the system can grow, become more organized where it can be labeled as a tropical depression with sustained winds of 62 km/h. Between 63 to 118 km/h, it is considered a tropical storm where after it reaches its status as a hurricane, it is then ranked on the Saffir-Simpson wind scale ranging from a category 1 (119 km/h) to a category 5 (>252 km/h) (Irish, 2008). Since 1842, 9 hurricanes have crossed over Long Island (Siverd, 2013) with some notable storms including, The Great New England Hurricane of 1938 (strongest storm to make landfall in New York history), Hurricane Carol in 1954, Connie and Diane in 1955, and Sandy in 2012 (Irish et al., 2008).

With regards to the physical dimensions of Jamaica Bay, the approximate area of the bay itself being 55.3 km^2 and a parameter of 40.1 km (Figure 2). The peninsula that partially encloses the bay has a length of 16 km (Siverd, 2013). Jamaica Bay is located in New York City, New York in the southwestern section of Long Island within New York City city limits (Figure 1a). Apart from natural influences, Jamaica Bay faces anthropogenic factors in its land loss. Over the past four decades, a significant amount of land has been lost due to navigational and construction dredging, pollution, and landfilling when Jamaica Bay was treated primarily as one large landfill for a growing city in the early 1900's (Waldman, 2008). These processes induced erosion across

the New York wetland. (Brash et al., 2011) Beginning in 1910, the main channel in Jamaica Bay was dredged from 5.5 m to 9.1 m (Swanson, 1992). These larger channels give more room for tidal influence and amplitude which is likely a factor in the wetland's erosion. The New York City Department of Environmental Protection has documented these issues with plans already in motion to restore the wetland platforms to its pre-1974 topography (Figure 1) (NYC-DEP, 2008).

Figure 1. a) (Top) Jamaica Bay and surrounding locations (Siverd, 2013); b) (Bottom) Jamaica Bay marsh loss from 1951 to 2003 (NPS, 2007).

(fig. cont'd.)

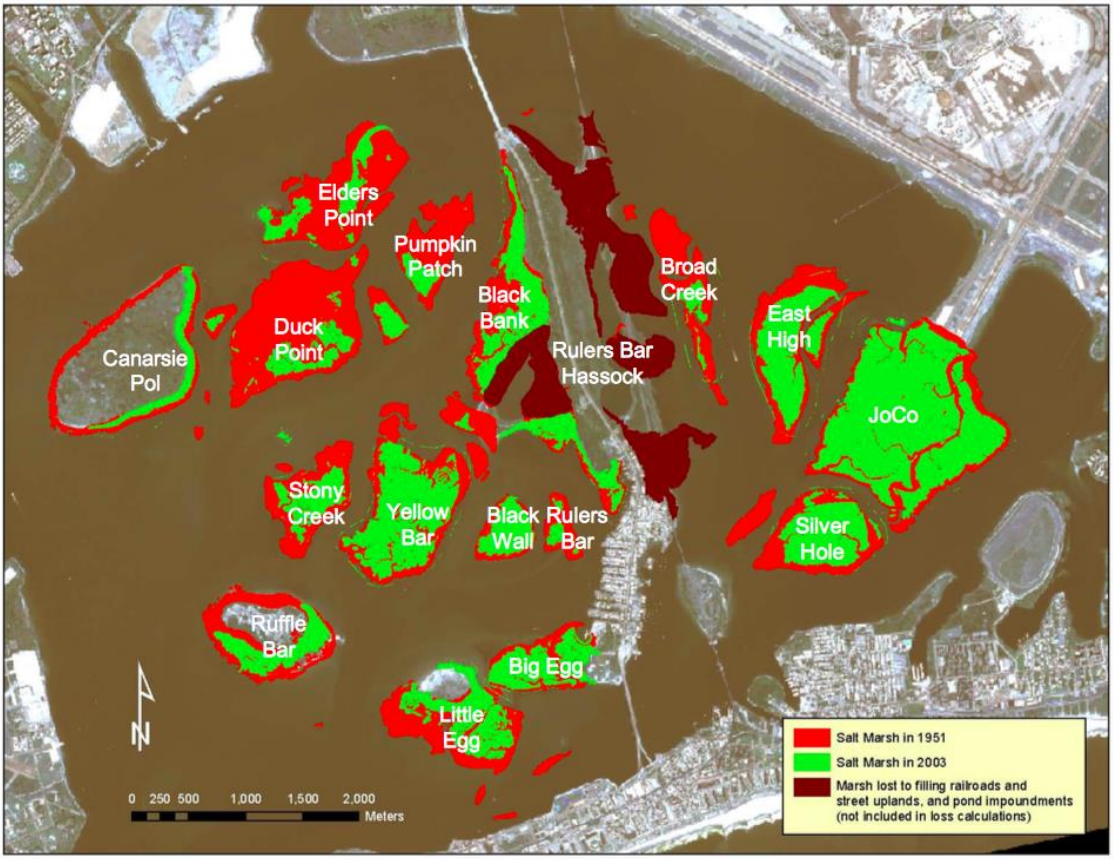

Dredging has played an important role in the continuation of providing open channels for ship navigation and landfill space in the bay itself. Dredging a marsh for the sediment to be used elsewhere without infilling what was taken can lead to increased erosion, change in sedimentation rate, sediment transport (Swanson & Wilson, 2008), reduced intertidal communities, and loss of bird breeding grounds (Siverd, 2013). This history of dredging in Jamaica Bay begins in 1904 with a 1.8 m deep by 15 m wide dredge in Canarsie Landing with all total major dredging activities resulting in over 9.6 km^2 of dredged earth at Jamaica Bay over the 104 years documented (Swanson & Wilson, 2008).

This study will focus on the role of vertical sediment accretion over the past century as a key control on the survival and decline of the Jamaica Bay saltmarsh, in the context of the influences described above. The aim is to evaluate relative contributions of mineral sediment

supply from documented hurricanes, nor'easters, and other mechanisms that produce flooding of the intertidal wetland platform (i.e. tides and waves). With this information, a sediment budget will then be constructed to identify what role these events play in the building or deterioration of this coastal salt marsh.

Salt Marsh Morphology, Sedimentation, and Processes

Salt marshes are vegetated intertidal flats that form in quiescent environments where the deceleration of sediment-laden waters is common. (Bloom and Stuvier, 1963; Redfield 1967, 1972; Allen et al., 1990). From this, sediment accumulates in sheltered waters like protected bays, estuaries, or other low-energy environments, resulting in tidal flats (Kearney and Turner, 2016).

Northeastern United States coastal salt marshes emerged after the post-glacial sea level rise decelerated between 4000 and 7000 years ago (Enos, 2015). Since then, many estuarine salt marshes have developed along the eastern North American coast, and have been observed as being highly productive (Hartig et al., 2002). However, in the last century, these wetlands have been eroding away with a decreasing rate of marsh production to support the wetlands with (Carey et al., 2017). This process can partially be attributed to natural variations in sea level rise within the last several thousand years, but the rate at which many coastal wetlands are deteriorating suggest larger and multiple factors are at play (Gornitz et al., 1995, 2001).

Relative sea level change is the sum of global eustatic sea level rise and subsidence (Vail et al., 1977; Kendall and Schlager, 1981; Antonioli et al., 2017). Coastal marshes and their relative elevation develop as equilibrium features, balanced between relative sea-level change and sediment supply (or erosion) (Roman et al., 1997). Marshes can grow vertically during a rise of relative sea level if sufficient organic and mineral deposition occurs (Morris et al., 2002).

Flooding to an appropriate level and frequency (also referred to as the hydroperiod) of the marsh stimulates root and leaf growth. This growth can also help trap mineral sediments, increasing elevation further and creating a more resilient wetland (French, 2006). In absence of deposition, the tidal flat becomes inundated to the point that plants will die, and the binding effects of plant roots diminish (Mudd et al., 2011). This may allow the mudflat to deteriorate and convert to open water (Allen et al., 1990).

Salt marsh inorganic sediment deposition can be documented stratigraphically (Cahoon et al., 2000) and can be seen within the soil record as horizontal laminations with interlaced sand/mud bedding (Letzch et al., 1980), unless bioturbated, in which case the bedding can be destroyed (Gardner and Porter, 2000). Inorganic sediment delivered to the marsh surface is often sourced from local subtidal areas, resuspended by waves and currents. Wave-current processes can be driven by periodic processes like tides, or episodic processes like storms (Nyman et al., 2006). Resulting marsh deposits are predominately fine-grained with the presence of sand and organic matter depending on the energy level and sediment sources during depositional events. Organic plant and bottom bay sediment material will settle onto the salt marsh in low energy environments or be produced in situ from plant production whereas sand will deposit mostly along marsh edges from resuspension or wave action from more high energy events such as storms and frontal systems (Stumpf et al., 1983; Pejrup et al., 2000).

Tidal sedimentation plays a dominant role in the growth and decay of wetlands. Generally, over millennial scales, marshes with rising sea-level through episodic flooding from storms and periodic tidal inundation, both which can deliver sediment. When the platform is flooded, suspended sediment can be deposited on the marsh platform (Leonard & Reed, 2002, Donnelly et al., 2004; Cahoon et al., 2006). This suspended load deposition is facilitated by the

vegetation on the marsh, which slows flow, aiding in deposition (Mudd, 2010). Wetlands proximal to open water and channels and at lower elevation tend to have larger sedimentation accumulation rates than higher locations more inland (~0.6 to 0.8 cm-yr^{-1} in a low marsh compared to ~0.2 to 0.3 cm-yr^{-1} in a high marsh) (Wolters et al., 2006, Fitzgerald et al., 2008). Tidal processes rarely create erosional surface unlike waves which can remove sediment and deposit it in offshore adjacent areas. Some of the eroded material can later be resuspended (by waves, tides, and currents) and recycled to marsh surfaces (Wilson and Allison, 2008; Wang et al., 2017; Hu et al., 2018).

Figure 2. Diagram of the boundary defining the different areas in a marsh platform (Fitzgerald et al., 2008)

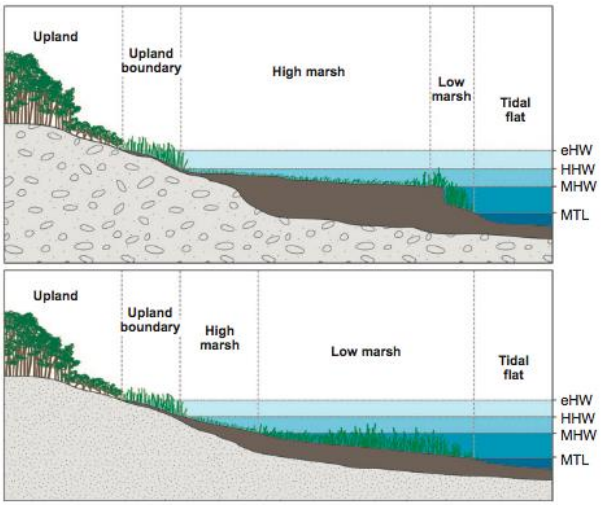

STUDY AREA

Geographical and Tidal conditions of Jamaica Bay

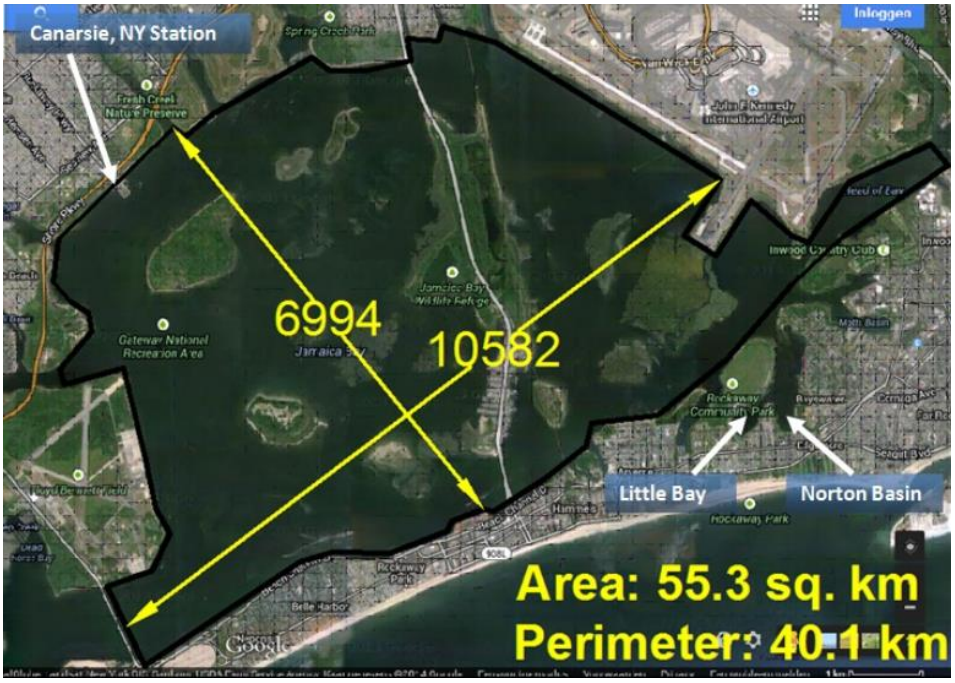

Figure 3. Physical parameters of Jamaica Bay (Siverd, 2013)

Jamaica Bay is one of the largest coastal ecosystems in the New York State area (Hart and Milken, 1992) **(**Figure 3). Located southeast of John F. Kennedy International Airport and south of Brooklyn and Queens, the central geographic coordinates of Jamaica Bay are 41°N, 74°W. Jamaica Bay is a part of the Gateway National Recreation Area that includes New Jersey and Staten Island. It is an estuary that includes open water, coastal shoals, bars, mudflats, low saltmarsh, high saltmarsh, and upland area. The relative proportion of this open water to land is 34% water to 66% land (NRDC, 2007). All of this provides a useful habitat for many species of birds, reptiles, and small mammals (Hartig et al., 2002).

The tidal dynamics of Jamaica Bay have become anthropogenically influenced due to extensive infrastructure development from 1907 to 1972 (Swanson & Wilson, 2008). Within the time period, Jamaica Bay went from 65.5 km^2 of marsh to 16.2 km^2, a reduction of more than

75%. (Siverd, 2013) (Figure 4). Natural and human impacts play a role in these alterations, but particular events are not well established. The modern tide range averages between 1.5 m and 1.6 m with an average bay depth of 4 m (NYC-DEP, 2014). Salinity in the bay varies from about 23 to 27 parts per thousand with fresh and salt water not mixing uniformly (NOAA, 2018).

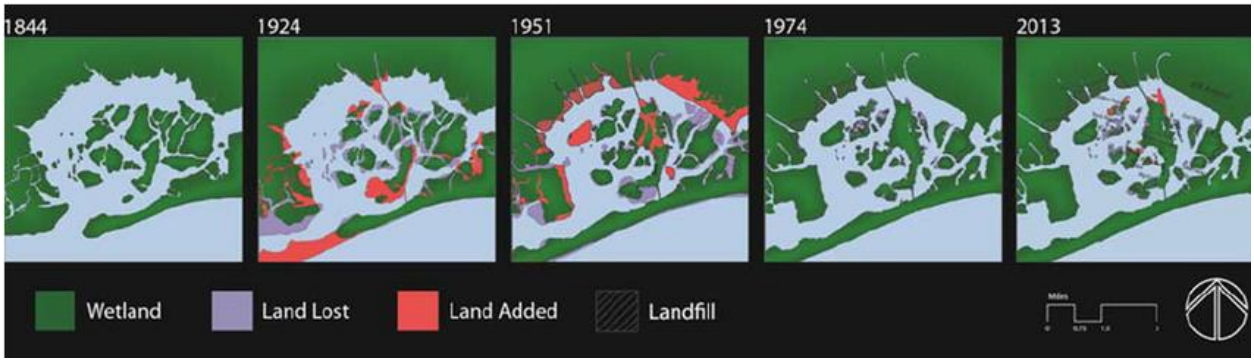

Figure 4. Marsh degradation in Jamaica Bay from 1844 to 2013 (Weis, 2015)

History of Geochronology in Jamaica Bay and Surrounding Areas

Vertical accretion in the Jamaica Bay salt marshes has been previous studied via geochronology using ^{210}Pb to obtain a sedimentation rate for the area (Zeppie, 1977; Kolker, 2005). Radionuclides such as ^{210}Pb are used to study and document an average annual input of sediment in marsh wetland (Zeppie, 1977; Hartig et al., 2002). Zeppie (1977) determined sediment accumulation rates from the Jamaica Bay wetland and found 0.5 to 0.8 cm-yr^{-1} sedimentation rate, based on ^{210}Pb as a radiochemical tracer for the geochronology. Kolker (2005) examined how the Jamaica Bay salt marsh responded to anthropogenic change in the past century and reported sediment accumulation rates on the order of 0.28 to 0.44 cm-yr^{-1}. These studies of wetland accretion in the area found a large amount of deterioration, erosion, anthropogenic influence, and many storm events layers within the sediment upon core analysis. Extensive marshland vertical accretion research has been done in New York as well as

surrounding states along the New England coast (Table 1). Orson (2008) reviewed over 50 papers to develop an overview of saltmarsh accretion rates along the mid-Atlantic coast:

The table below shows New York and most other nearby salt marsh area aligning with the sedimentation accumulation rates found by Kolker (2005) and Zeppie (1977) in the Long Island

Table 1. Overview of Saltmarsh Vertical accretion rates in New England (Orson, 2008) area.

State	Vertical Accretion (mm/yr)	Standard Deviation (mm/yr)	# of Studies in the Area	Tracers Used
New York	3.45	1.24	21	^{210}Pb
New Jersey	8.13	4.5	3	^{210}Pb, ^{137}Cs, Pollen, Historical
Delaware	5.29	2.25	23	^{210}Pb, ^{137}Cs, Radiocarbon Dating
Virginia	3.4	5.29	5	Surface Elevation Table
Maryland	2.89	13.4	16	^{210}Pb, ^{14}C, ^{137}Cs, Pollen dating

Bedrock Geology of Study Area

Jamaica Bay lies at the southern portion of Long Island in Queens, New York. The initial formation event of the modern day landscape of the area is Wisconsinan glaciation 85,000 to 110,000 years ago creating the Ronkonkoma terminal moraine and its outwash plain (Lewis et al., 1991). The plain is made from melted glacial water that flowed and deposited sediments under the glacier to the end point of the glacier causing a flat plain. The deposits are of poorly sorted, unconsolidated clay, silt, sand, and gravel of Late Cretaceous and Pleistocene age

(Merguerian et al., 2010). Under these sediments lie the Magothy Formation of unconsolidated sands interbedded with silts and clays with a thickness of 305 m. The bottom 30 m of this formation has coarser deposits of silts and clay. The Magothy Formation formed during a mid-Turonian (90 mya) eustatic lowering of sea level. Generally, the sediments consist of sands and silty clays representing upper delta plain, lower delta plain, and delta front environments during sedimentation (Van Sickel et al., 2004).

Below the Magothy formation is the Raritan formation with a thickness of 91 m with a primary rock type of clay or mud (Christopher et al., 1979). Both the Magothy and the Raritan formations are a part of the Monmouth Group in south Long Island where Jamaica Bay lies and are of Upper Cretaceous age. Lastly, the basement geology of Long Island is Gneissic metamorphic rocks formed from a continental collision ~1 billion years ago in the Precambrian (Uchupi et al., 2000).

STATEMENT OF PROBLEM AND OBJECTIVES

Hurricanes and strong winter storms play a factor in the vertical accretion of Jamaica Bay salt marshes and potentially play a role in the lateral erosion of these same salt marshes. This study aims to clarify the relative roles of hurricanes and extra-tropical storm in supplying sediment for vertical accretion in the Jamaica Bay wetlands. This will be accomplished by the integration of storm records, ^{137}Cs and ^{210}Pb geochronology, and mineral content across 12 cores collected across Jamaica Bay in Far Rockaway, New York. This study will focus on the integration between peaks in mineral accumulation downcore and historical documented storm events to determine the relative mineral contribution of these events to the general sediment budget in Jamaica Bay on the salt marsh platform. The study will consist of identifying layers as elevated mineral sediment content and relating them to known storm landfalls. Lastly, these storm deposit events will be documented spatially and temporally to find a wider context to compare with other forms of sedimentation in the area.

METHODS

Sample Collection and Mineral Peak Analysis

USGS collected 12 sediment cores across the Jamaica Bay wetland in August of 2014. These cores were taken on the islands of East High, JoCo, Blank Bank, Big Egg, Little Egg, Four Sparrow, Duck Point, Yellow Bar, Spring Creek, Fresh Creek, Stony Creek, and Ruffle Bar in the Recreation Area (Figure 3).

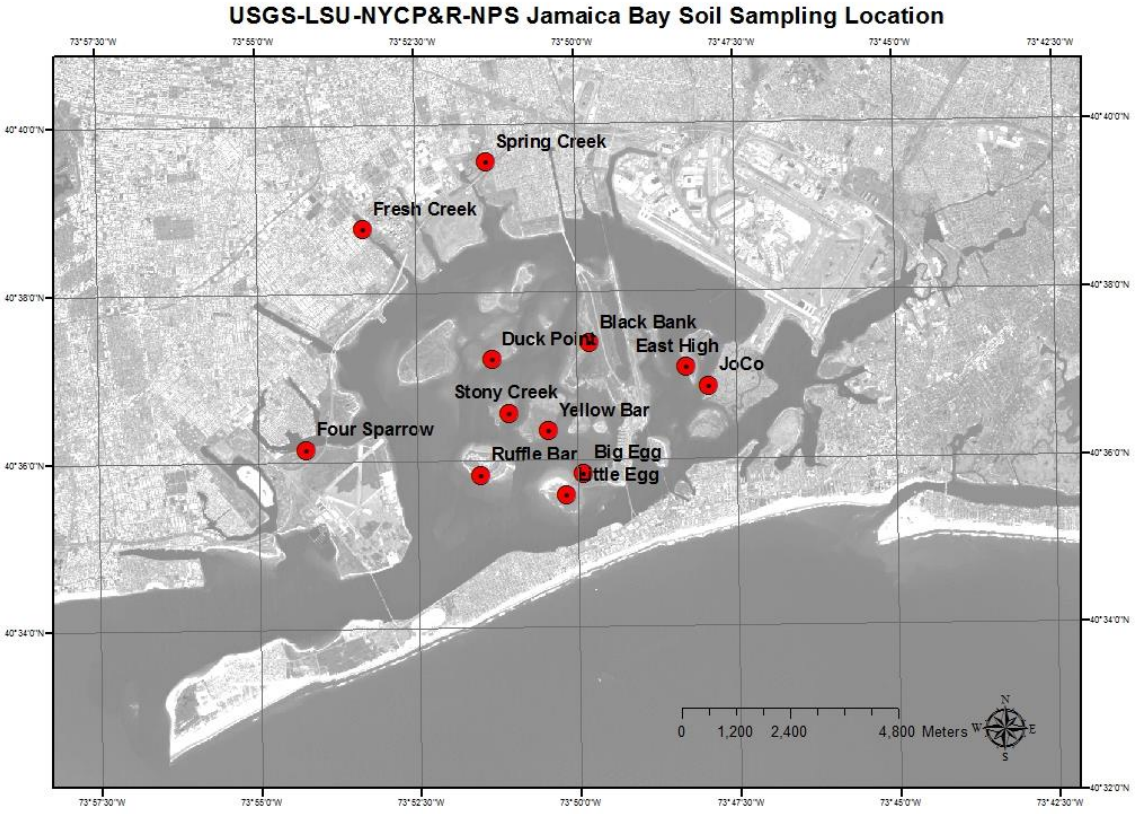

Figure 3. Core sites throughout Jamaica Bay (Source: Hongqing Wang, USGS)

Cores were collected by inserting a thin walled aluminum pipe "T-core" (10 cm in diameter x 60 cm in length) into the marsh. Cores were kept frozen prior to processing in the Louisiana State University Geology and Geophysics department, likely leading to expansion of water volume in cores during freezing. Partially thawed cores were extruded, measured, and

sliced into 2 cm intervals using an industrial band-saw. Intervals were further divided radially into two subsamples of known volume: 75% of the material was reserved for radiochemistry, and 25% for total organic fraction, mineral fraction, and dry bulk density analysis.

Organic (Φ_C) and mineral (Φ_S) fractions were determined using standard loss-on-ignition methods (Equations 1 and 2) (Heiri et al., 2001). Dry bulk density (ρ_b, g-cm^{-3}) was derived from the mass and total volume of the sample after drying the sample at 105°C for 24 hours (Eq. 3).

(1)

$$\Phi_c = \frac{Combusted\ sample\ mass\ (2\ hours\ @\ 550\ ^\circ C)}{Dry\ sample\ mass\ (24\ hours\ @\ 60\ ^\circ C)}$$

(2)

$$\Phi_s = (1 - \Phi c)$$

(3)

$$\rho_b = \frac{Dried\ sample\ mass\ (24\ hours\ @\ 105^\circ C)}{Sample\ volume}$$

Mineral accumulation mass per layer (m_L, g-cm^{-2}) was then determined from:

(4)

$$m_L = \Phi_s * \rho_b * \Delta_z$$

where Δz is 2 cm, or the layer thickness after Smith et al. (2015). Core profiles of m_L were used to calculate whole-core mineral accumulation averages ($\overline{mL}$) and standard deviations (σ_{mL}) of mineral and organic composition after Smith et al. (2015).

Geochronology

The larger subsample of each interval was reserved for determination of sediment accumulation rates (SARs) using gamma spectrometric analyses. Radionuclides of interest are ^{210}Pb (natural ^{238}U series, $t_{1/2}$=22.2 years), and ^{137}Cs (anthropogenic fallout, $t_{1/2}$=30.1 years). Data are reported in decays per minute per gram dry sediment (dpm/g), for which 1 dpm=60 Bq. Water content was determined gravimetrically in samples for radionuclide analysis. Dried samples were then ground using a mortar and pestle, and sealed into petri dishes. Samples for ^{210}Pb analysis rested in sealed dishes for 14 days before ^{210}Pb data were collected, to allow ingrowth of ^{210}Pb parent radionuclide ^{222}Rn and to determine supported activities (Corbett, 2015).

All samples were analyzed on Canberra LEGe 3825 and 2020 detectors calibrated for energy and efficiency using standard reference materials (from US National Institute of Standards and Technology, and International Atomic Energy Agency), with samples from a single core being restricted to one detector. Sample self-absorption for ^{210}Pb gamma emissions was determined using the transmission method (Cochran and Masqué, 2003). Activities associated with the 295 and 352 keV peaks of ^{214}Pb and the 609 keV peak of ^{214}Bi were averaged to determine the amount of supported ^{210}Pb. The supported ^{210}Pb activity is then subtracted from total ^{210}Pb activity to determine excess ^{210}Pb ($^{210}Pb_{xs}$) activity. Activities for ^{137}Cs were determined from analysis of the 661 keV peak (Cunha et al., 2001).

Differentiation of ^{210}Pb Geochronology Models

^{210}Pb can be used as a tool for geochronological reconstruction by creating an age model based on a range of assumptions regarding the supply of ^{210}Pb and sediment from the water column to the sediment surface. The general assumptions are: ^{210}Pb is quickly removed from the

atmosphere and freshwater streams and sequestered in soils in sediments; ^{210}Pb is immobile once deposited; excess ^{210}Pb does not migrate down the sediment column; supported ^{210}Pb is in secular equilibrium with its grandparent ^{226}Ra; and supported ^{210}Pb is independent of depth (Corbett, 2015).

The Constant Flux, Constant Sediment (CFCS) model assumes an increased flux of sedimentary particles from the water column will remove proportionally increased amounts of ^{210}Pb from the water to the sediments (Appleby, 1983). The model also assumes that vertical sediment accumulation rate will not affect the ^{210}Pb concentration and it will remain constant throughout time. Some discrepancies found by Appleby (2001) within the CFCS model indicate variations in the initial ^{210}Pb concentration that will remain constant can be due to a specific event such as a flood, storm, slump, or anthropogenic activity which is not the norm as sedimentation continues.

The excess ^{210}Pb concentration will vary with depth in accordance with the formula (Appleby and Oldfield 1983):

(5) $$\frac{C}{Co} = e^{-\lambda t}$$

where C_o is the unsupported ^{210}Pb concentration of sediments at the sediment water interface and the radioactive decay constant (λ) of ^{210}Pb is:

(6) $$\lambda^{210}\text{Pb} = log2/22.26 = 0.0311y^{-1}$$

(7) Or λ^{210}Pb = $ln(2/22.26y) = 0.03114y^{-1}$, as previously stated

According to Appleby and Oldfield (1983), the age of sediment layers with ^{210}Pb concentration C is therefore:

(8) $$t = 1/-\lambda \ln(C/C_o)$$

Long-term sediment accumulation rates for ^{210}Pb using the CFCS model were calculated using Sigmaplot© by least-squares regressions on radionuclide data based on Eq. 2 from Muhammad et al. (2008) adapted from Nittrouer and Sternberg (1981):

(9)

$$A_z = A_0 e^{(-\frac{\lambda z}{S})}$$

where A_z is activity at depth z (dpm/g), A_0 is activity extrapolated to the sediment surface (dpm/g), λ is the decay constant of radionuclide of interest (year^{-1}), and *S* is the sediment accumulation (long term, ^{210}Pb) rate.

The constant rate of supply (CRS) or the constant flux model is designed to determine the age of a given depth from a ^{210}Pb vertical profile downcore. The model assumes that excess ^{210}Pb is supplied a constant rate to sediments, initial ^{210}Pb concentration in the sediment is variable, as well as the accumulation rate (Turner et al., 1996). Because this model assumes constant ^{210}Pb atmospheric fallout, no post-depositional mixing is also assumed. An assumption that makes the CRS model more applicable to this study is that the transport parameters are independent of sedimentation rate. All of this allows for the CRS model to have a variable sedimentation rate (Corbett, 2015).

According to Appleby and Oldfield (1978), the initial concentration *Co(t)* of excess ^{210}Pb in sediment of age *t* years must satisfy the following:

(10) $$C_o(t)\, r(t) = constant$$

where $r(t)$ (g/cm^{2}yr^{-1}) is the dry mass sedimentation rate at time t.

From this equation, Appleby and Oldfield (1978) developed a relation for the age of deposit at depth x:

(11) $$t=(1/\lambda)\ln(I_0/I_x)$$

^{137}Cs Geochronology Methods

For the ^{137}Cs geochronology, SARs for each core were calculated using Equation 12, where Z_{max} is the ^{137}Cs peak depth and T is the year of sample collection (Nittrouer et al., 1983). This equation assumes negligible bioturbation due to the clear ^{137}Cs profiles and peaks throughout the cores.

(12)

$$\text{SAR} = \frac{\boldsymbol{Z_{max}}}{\boldsymbol{T - 1953}}$$

^{137}Cs initial activity value is correlated to 1953, the year sub-atmospheric nuclear testing began and when ^{137}Cs fallout began. When sun-atmospheric testing reached its peak, this year has been correlated to 1963. From this, another SAR can be found in a similar manner as Equation 12.

(13)

$$\text{SAR} = \frac{\boldsymbol{Z_{max}}}{\boldsymbol{T - 1963}}$$

Combining Geochronology and Mineral Mass Variations to Determine Storm-Sediment Contributions

Core mineral content and geochronology indicated down-core peaks in mineral content that were apparently consistent in absolute age for several cores. To allow more detailed spatio-temporal study of variations in mineral content, the following method was used to identify and develop age models for subsurface maxima in mineral content after Smith et al. (2015). To standardize the peak identification process, in each core, peaks in mineral content were defined as depth ranges when $m_L > \overline{m_L}$ where "m_L" is defined as mineral mass layer and "$\overline{m_L}$" is defined as average mineral mass layer. Year of deposition Year_{peak} and uncertainty of Year_{peak} were estimated from Equations 14 and 15:

(14) $$\text{Year}_{\text{peak}} = \text{Year}_{\text{collection}} - \frac{Depth\ peak}{SAR\ Avg}$$

(15) $$\text{Uncertainty} = \frac{\Delta z}{SAR\ Avg}$$

The combined year of deposition and uncertainty for each peak then defined a window of time that was compared to known chronologies of storms passing over or near to the study area. A table of all tracked extra-tropical storms and hurricanes that fell within a 200 km radius of the Jamaica Bay estuary system was created using the NOAA hurricane tracker database (NOAA, 2017). Hurricane Sandy's storm radius of 1609 km was used as a reference point to gauge the likelihood of capturing storms that effected the study area in this chosen radius (Brandon et al., 2014). Previous studies (Denommee et al., 2014; Smith et al., 2015) have used a 100 km radius, but produced an unreasonably small number of potential events. Hence, the search radius was

increased. Peaks in mineral mass were then assigned to known documented storms if their determined age window contained the landfall year of a particular storm (Denommee et al., 2014).

Storm Mass Contributions

Mineral mass peaks were rarely restricted to one interval, and were often defined by more than two depth points. Three equations were used to define the mineral mass contribution of each recognized storm event layer in a statistically robust way (Equations 16, 17, and 18). Equation 16 defines Σ_{min} as the summation of mineral mass layer values within a single event layer that exceed the average value of a single core. Equation 17 defines Σ_{max} as the summation of values that exceed the sum of the whole-core average and standard deviation ($\overline{mL} + \sigma_{mL}$). Equations 16 and 17 serve to bracket reasonable minimum and maximum values of mineral mass contribution per event layer within a single core, and Equation 18 is the average of these two values, allowing representation of the sediment mass within each peak as a mean ± uncertainty.

(16)

$$\Sigma_{min} = \sum_{i=\,mL>\overline{mL}}^{mL\ peak\ intervals} imL$$

(17)

$$\Sigma_{max} = \sum_{i=\,mL>\overline{mL}+\sigma mL}^{mL\ peak\ intervals} i\overline{mL}$$

(18)

$$\Sigma_{mL} = \left(\frac{\Sigma\,\max + \Sigma\,min}{2}\right) \pm \left(\frac{\Sigma\,\max - \Sigma min}{2}\right)$$

RESULTS

Identification of Storms That Have Impacted the Area During the Last 159 Years

Figure 4 and Table 2 show the tracks, timing, and storm descriptions for all storms that tracked within 200 km of the study area during the past 159 years, based on data from NOAA (2017). A total of 24 storms were identified in 28 mineral mass peaks with 14 of those being categorized as a hurricane and the other 11 being tropical storms and depressions that later transitioned into extra-tropical storms. In total, 17 storms documented underwent extra-tropical transition (Figure 4).

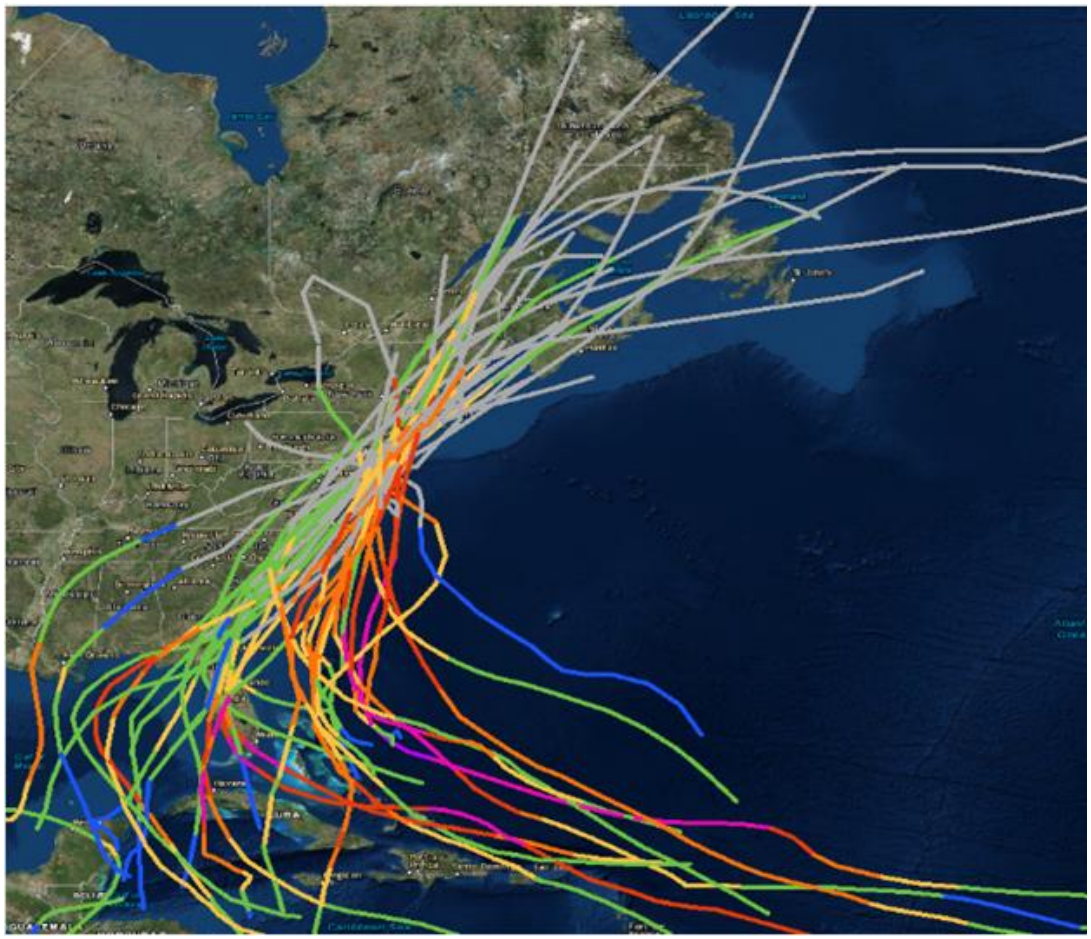

Figure 4. All storm tracks fallen within the 200 km radius of Jamaica Bay (NOAA, 2017)

Table 2. All documented Hurricanes and Extra-tropical storms in a 200 km of Jamaica Bay (NOAA, 2017)

Storm Name	Date	Type/Maximum Intensity	Type/Intensity within 200 km Radius
ANDREA 2013	Jun 05, 2013 to Jun 08, 2013	Tropical Storm	Extra-tropical Storm
SANDY 2012	Oct 21, 2012 to Oct 31, 2012	Category 3	Extra-tropical storm
IRENE 2011	Aug 21, 2011 to Aug 30, 2011	Category 3	Tropical Storm
BARRY 2007	May 31, 2007 to Jun 05, 2007	Tropical Storm	Extra-tropical storm
TWENTY-TWO 2005	Oct 08, 2005 to Oct 14, 2005	Tropical Depression	Extra-tropical storm
CINDY 2005	Jul 03, 2005 to Jul 11, 2005	Category 1	Extra-tropical storm
CHARLEY 2004	Aug 09, 2004 to Aug 15, 2004	Category 4	Extra-tropical storm
GORDON 2000	Sep 14, 2000 to Sep 21, 2000	Category 1	Extra-tropical storm
BOB 1991	Aug 16, 1991 to Aug 29, 1991	Category 2	Category 2
GLORIA 1985	Sep 16, 1985 to Oct 02, 1985	Category 4	Category 1
BELLE 1976	Aug 06, 1976 to Aug 10, 1976	Category 3	Category 1
DONNA 1960	Aug 29, 1960 to Sep 14, 1960	Category 4	Category 2
CAROL 1954	Aug 25, 1954 to Sep 01, 1954	Category 3	Category 3
Homestead Florida Hurricane of 1945	Sep 12, 1945 to Sep 20, 1945	Category 4	Tropical Depression

(table cont'd.)

Storm Name	Date	Type/Maximum Intensity	Type/Intensity within 200 km Radius
Cuba-Florida Hurricane of 1944	Oct 12, 1944 to Oct 24, 1944	Category 4	Never made Landfall
1944 Great Atlantic Hurricane	Sep 09, 1944 to Sep 16, 1944	Category 4	Category 1
New England Hurricane of 1938	Sep 09, 1938 to Sep 23, 1938	Category 5	Category 3
Hurricane Seven 1934	Sep 05, 1934 to Sep 10, 1934	Category 2	Tropical Storm
Tropical Storm Eight 1924	Sep 27, 1924 to Oct 01, 1924	Tropical Storm	Tropical Storm
Tropical Storm One 1916	May 13, 1916 to May 18, 1916	Tropical Storm	Extra-tropical Storm
Hurricane One 1915	Jul 31, 1915 to Aug 05, 1915	Category 1	Extra-tropical Storm
Tropical Storm One 1907	Jun 24, 1907 to Jun 30, 1907	Tropical Storm	Extra-tropical Storm
Hurricane Two 1904	Sep 08, 1904 to Sep 15, 1904	Category 2	Extra-tropical Storm
Hurricane Three 1903	Sep 12, 1903 to Sep 17, 1903	Category 1	Category 1
UNNAMED 1902	Jun 12, 1902 to Jun 17, 1902	Tropical Storm	Extra-tropical Storm
Tropical Storm Six 1900	Oct 10, 1900 to Oct 15, 1900	Tropical Storm	Extra-tropical Storm
Hurricane Nine 1899	Oct 26, 1899 to Nov 04, 1899	Category 2	Extra-tropical Storm
The Florida Panhandle Hurricane of 1894	Oct 01, 1894 to Oct 12, 1894	Category 3	Category 1
New York Hurricane of 1893	Aug 15, 1893 to Aug 26, 1893	Category 3	Category 1

(table cont'd.)

Storm Name	Date	Type/Maximum Intensity	Type/Intensity within 200 km Radius
Tropical Storm Five 1888	Sep 06, 1888 to Sep 13, 1888	Tropical Storm	Extra-tropical Storm
Great Beaufort Hurricane of 1879	Aug 13, 1879 to Aug 20, 1879	Category 3	Category 1
Hurricane Four 1877	Sep 21, 1877 to Oct 05, 1877	Category 3	Extra-tropical Storm
New England Gale of 1869	Sep 07, 1869 to Sep 09, 1869	Category 3	Category 3
Tropical Storm 1866	Oct 29, 1866 to Oct 30, 1866	Tropical Storm	Extra-tropical Storm
Hurricane Three 1858	Sep 14, 1858 to Sep 17, 1858	Category 2	Category 1

SAR Results Using ^{137}Cs, and ^{210}Pb CFCS and CRS Models

Radioisotope profiles are shown in Figures 5a-5l. Plots of depth versus age using the ^{210}Pb CRS model are shown in Figures 6a-6l. SAR results for the geochronological models using ^{137}Cs, ^{210}Pb, CFCS, and CRS approaches are shown in Table 3.

Across all cores and methods, the sediment accumulation rate ranged from 0.22 to 0.83 cm-yr^{-1} with the largest range within an isolated method being the ^{137}Cs 1963 SAR, but seems to be consistent with all other methods and smallest being ^{210}Pb CRS SAR (Table 3). With respect to age models, the two ^{210}Pb models carried generally a larger sediment accumulation rate than SARs estimated from ^{137}Cs. Once averaged, the CRS model was .46 cm-yr^{-1} with the CFCS

model having an average SAR rate of 0.5 cm-yr^{-1}. The ^{137}Cs based sediment accumulation rates for Jamaica Bay marshes are in the range of 0.4-0.7 cm-yr^{-1} (Table 3).

With respect to specific cores, Little Egg and Duck Point carries the highest SARs of 0.7 cm-yr^{-1} and 0.72 cm-yr^{-1} respectively from the average of all four methods. Little Egg, however, was only cored to a depth of 27 cm, the shortest core of this study. The lowest SAR found in the cores is 0.39 cm-yr^{-1}; a value found at Four Sparrow, Yellow Bar, Spring Creek, and Fresh Creek. The most agreeable core between all methods is JoCo with a range of 0.09 cm-yr^{-1} and the most disagreeable core being Black Bank with a range of 0.88 - 0.68 cm-yr^{-1} (Table 3). In this case, the low ^{137}Cs activity and single detected sample makes the Cesium suspect. The average of all cores is 0.48 cm-yr^{-1}.

In order to apply our approach to estimating the age of each mineral event layer to this data set, a single SAR is necessary for each core. In most cases SARs by all methods fall within a range of 0.15 cm-yr^{-1} (excepting Black Bank, which has very low ^{137}Cs activities that may not yield a reliable chronostratigraphy; Fig. 5j, Table 3). For the purposes of simplicity, an average of the CFCS, CRS, and ^{137}Cesium 1963 and 1953 model SARs was calculated for each core, and used to develop age models for event layers.

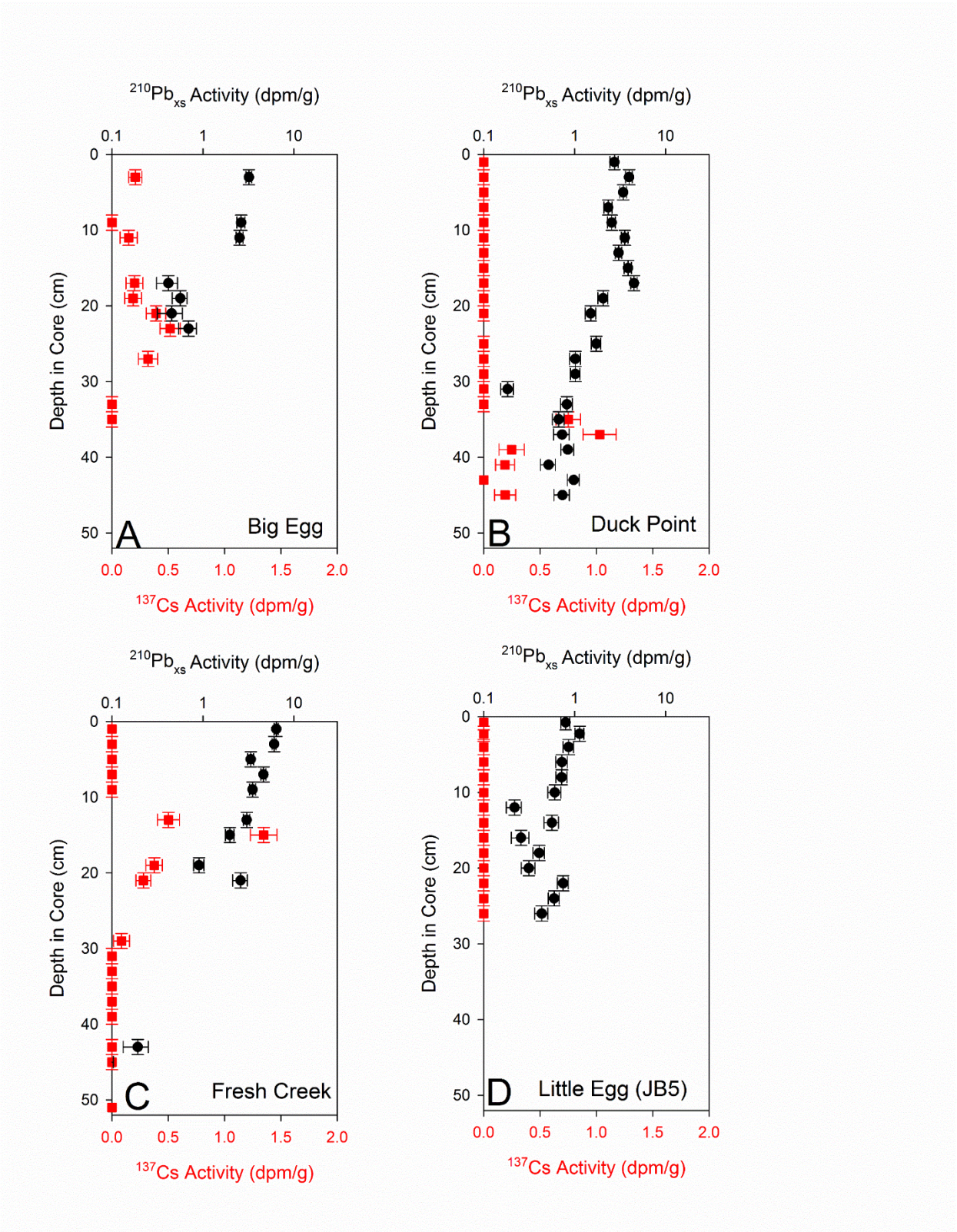

Figure 5. ^{137}Cs and ^{210}Pb Activity profiles downcore for Big Egg (a), Duck Point (b), Fresh Creek (c), and Little Egg (d).

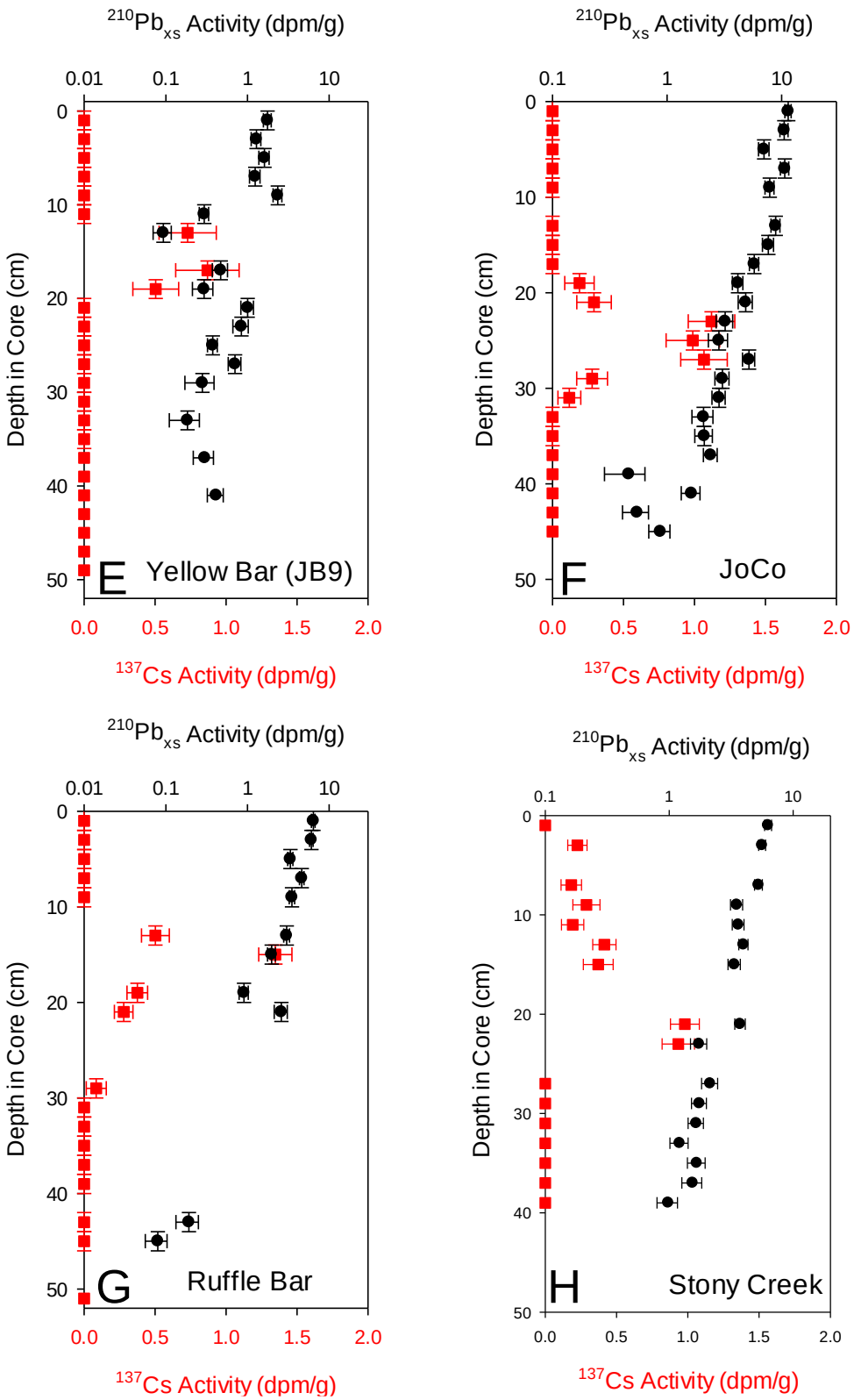

Figure 5 (cont.). ^{137}Cs and ^{210}Pb Activity profiles downcore for Yellow Bar (e), JoCo (f), Ruffle Bar (g), Stony Creek (h).

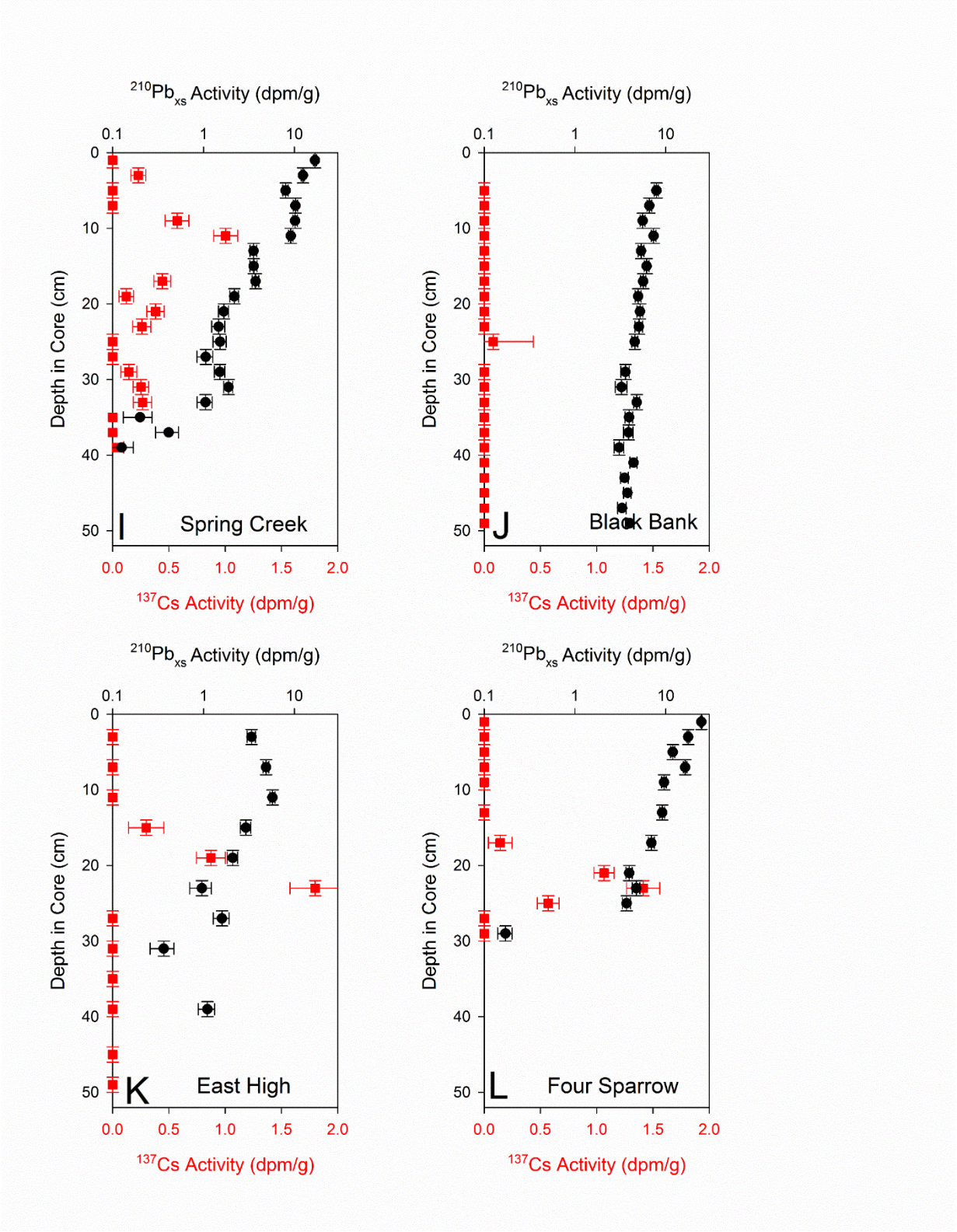

Figure 5 (cont.) ^{137}Cs and ^{210}Pb Activity profiles downcore for Spring Creek (i), Blank Bank (j), East High (k), and Four Sparrow (l).

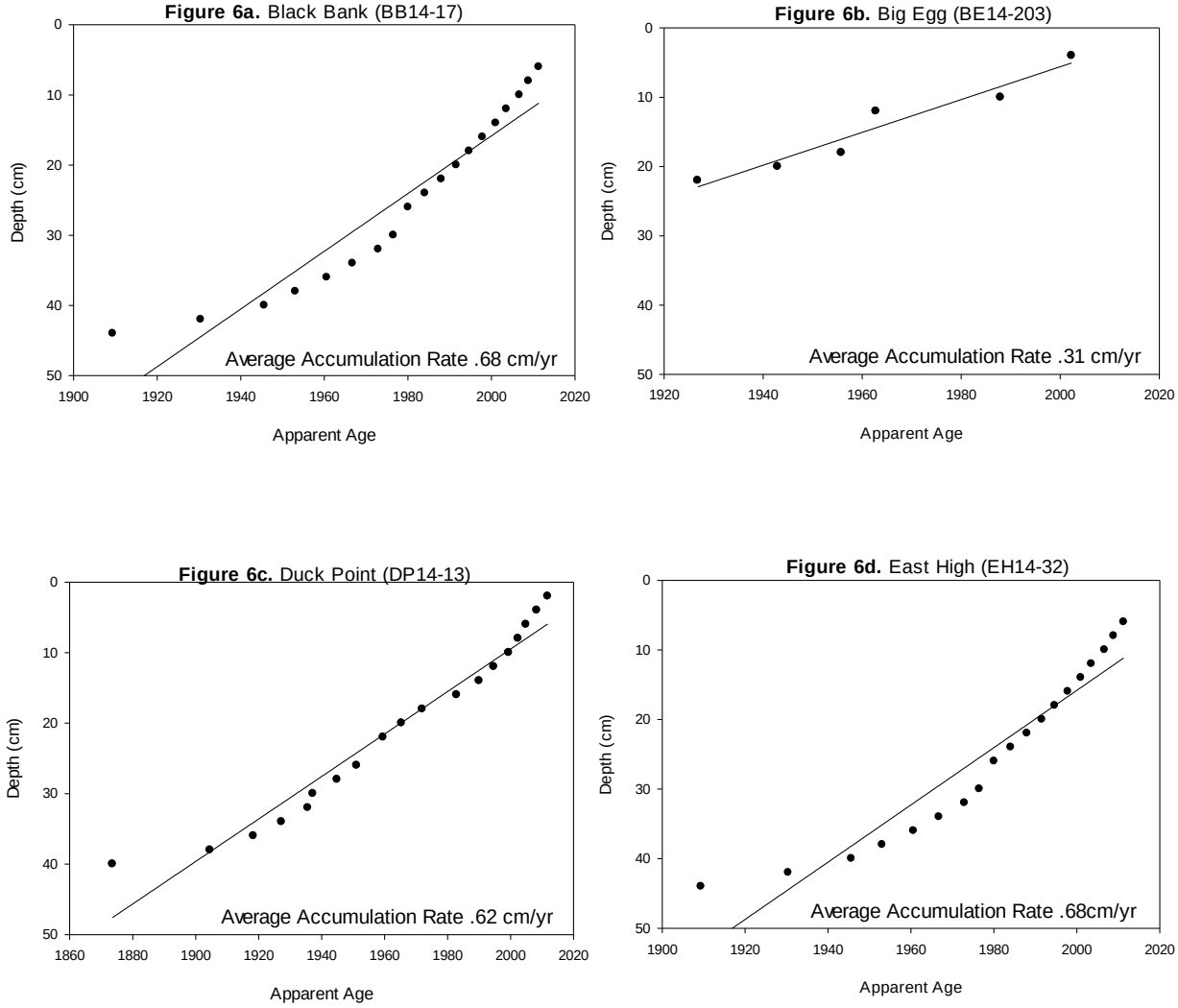

Figure 6. CRS model for cores Black Bank (a), Big Egg (b), Duck Point (c), and East High (d). Showing apparent age versus depth.

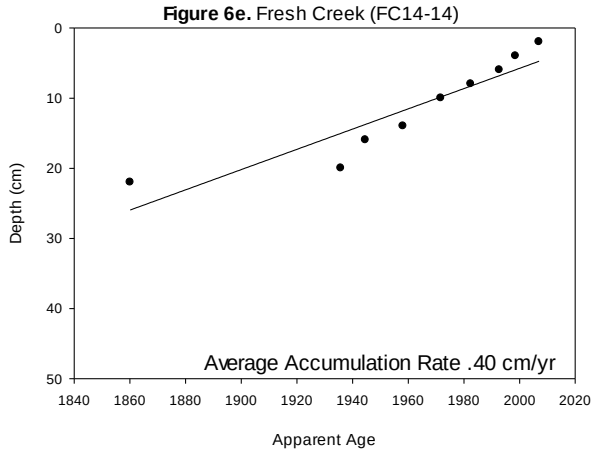

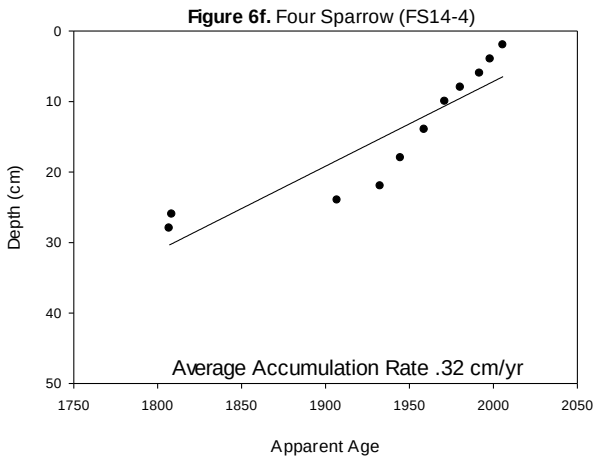

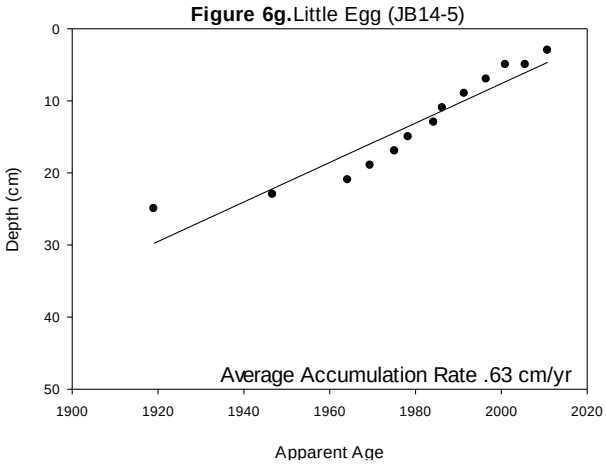

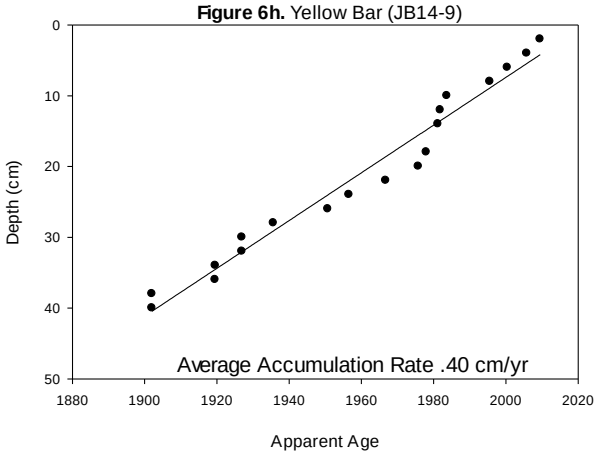

Figures 6 (cont.). CRS model results for cores Fresh Creek (a), Four Sparrow (b), Little Egg (c), and Yellow Bar (d). Showing apparent age versus depth.

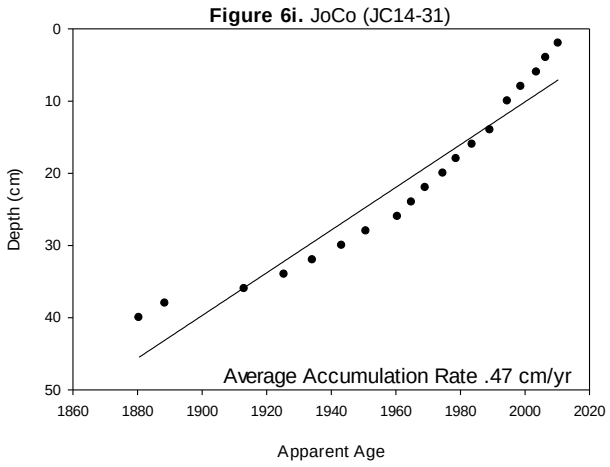

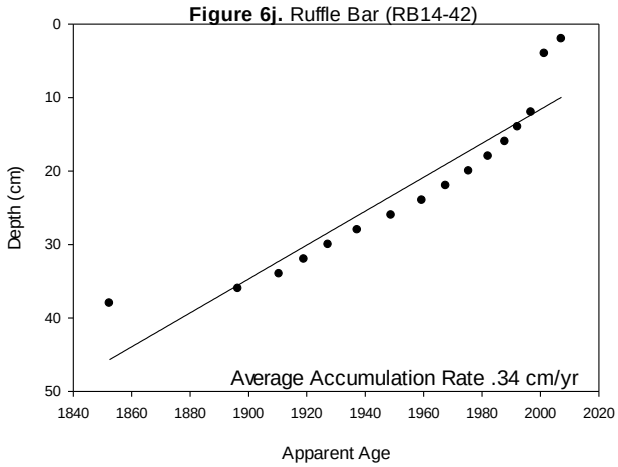

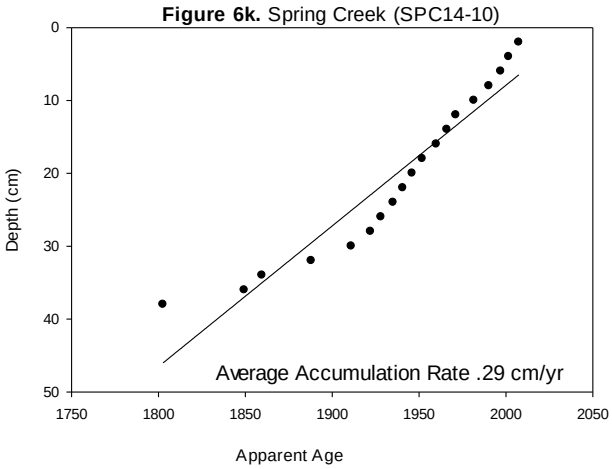

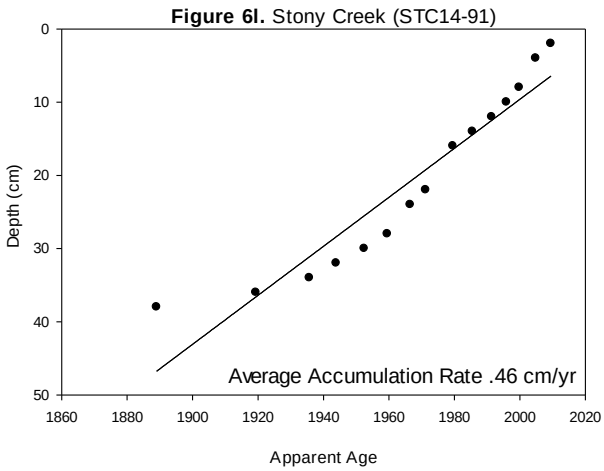

Figure 6(cont.) CRS model results for JoCo (i), Ruffle Bar (j), Spring Creek (k), and Stony Creek (l) showing apparent age versus depth

Table 3. Sediment Accumulation Rates (SAR) with each core for each geochronology method used.

Core Sites	Latitude	Longitude	Core Max Depth (cm)	SAR mean w/ CFCS model (cm-yr^{-1})	CFCS Uncertainty in years	R^2	SAR mean w/ CRS model (each core averaged) (cm-yr^{-1})	CRS Uncertainty in years	^{137}Cs 1963 peak depth (cm)	^{137}Cs SAR (cm-yr^{-1})	^{137}Cs 1953 Max Depth (cm)	^{137}Cs 1953 SAR (cm-yr^{-1})	Mean SARs (cm-yr^{-1})	Standard Deviation (cm-yr^{-1})	Inconsistent SARs	Elevation (cm)
East High	40.618° N	73.805°W	50	0.51	3.92	0.61	0.68	2.94	23	0.45	27	0.44	0.52	0.14		79
JoCo	40.614° N	73.799°W	46	0.55	3.63	0.89	0.46	4.35	25	0.49	31	0.51	0.5	0.04		81
Blank Bank	40.623° N	73.830°W	50	0.88	2.27	0.77	0.68	2.94	Nd	Nd	Nd	Nd	Nd	0.14	xx	31
Big Egg	40.597° N	73.832°W	48	0.42	4.76	0.83	0.31	6.45	23	0.45	27	0.44	0.41	0.06		68
Little Egg	40.593° N	73.863°W	27	0.83	2.41	0.43	0.62	3.23	Nd	Nd	Nd	Nd	xx	0.15	xx	55
Four Sparrow	40.602° N	73.904°W	40	0.41	4.88	0.92	0.3	6.67	23	0.45	25	0.41	0.39	0.06		82
Duck Point	40.620° N	73.855°W	46	0.77	1.54	0.63	0.62	3.17	37	0.73	45	0.74	0.72	0.07		2
Yellow Bar	40.606° N	73.841°W	50	0.4	5	0.5	0.4	5	17	0.33	19	0.31	0.36	0.05	xx	40
Spring Creek	40.659° N	73.856°W	40	0.4	5	0.92	0.28	7.14	11	0.22	39	0.64	0.39	0.19		89
Fresh Creek	40.646° N	73.889°W	54	0.4	5	0.9	0.4	5	15	0.29	29	0.48	0.39	0.08		86
Stony Creek	40.609° N	73.851°W	40	0.51	3.92	0.92	0.46	4.35	21	0.41	25	0.41	0.45	0.05		59
Ruffle Bar	40.597° N	73.859°W	54	0.49	4.08	0.95	0.33	6.06	25	0.49	29	0.48	0.45	0.08		67
Averages				0.55			0.46			0.44		0.48	0.48			62

Identification of Event Layers and Matching Layers to Specific Events

Most cores were found to be organic-rich, marked with irregularly distributed cm-scale beds having increased mineral content (Figure 7a-l). Historic storm data, dating as far back as the late 1800's, were used to identify hurricanes and major winter storms determined by the National Weather Service passing within 200 km of the study area (Table 2). Nor'easters were not documented or correlated in this study due to NOAA's historical storm tracker not including a robust model of tracking nor'easters specifically to then align into our radius. Strength nor location tracking could be found in an archival sense unlike hurricanes and other tropical systems. Likely storm-event deposits in each core were identified as layers with mineral content higher than the core mean plus one standard deviation and were matched to historic events via radioisotope geochronology, incorporating age-model uncertainty (Table 3) adapted from Smith et al., 2015. Overall, 24 out of the 28 defined storm layers match the timing of historic strong storms (within uncertainty ranging from 2 to 5 years) from 1858 to Hurricane Sandy in 2012 (Tables 4.1 and 4.2). Some notable storms documented within the cores are Hurricane Sandy, Irene, Bob, Gloria, Belle, Carol, the 1944 Great Atlantic hurricane, and the New England Hurricane of 1938. Years of largest activity in terms of documented events are 2005 (3), 1985 (3), and 1934 (3). (Table 4.1 and 4.2). Fresh Creek's core documents the most events (5), with all peaks in the core documented within 1945 and 1877. The core with the least number of events documented is Spring Creek (1) with only Hurricane Sandy documented in core (Table 4.1). The core with the largest mineral accumulation for its specific events is Little Egg with a total storm mineral accumulation of 5.41 g/cm^2 (Table 4.2). The event that deposited the largest amount of sediment is Hurricane Gloria in 1985 found in the Little Egg core with a total mineral accumulation of 2.73 g/cm^2 (Table 4.1). The event that deposited the least amount of sediment,

but still considered an event, is Hurricane Sandy found in the Spring Creek core with a mineral accumulation amount of .069 g/cm^2. (Table 4.1)

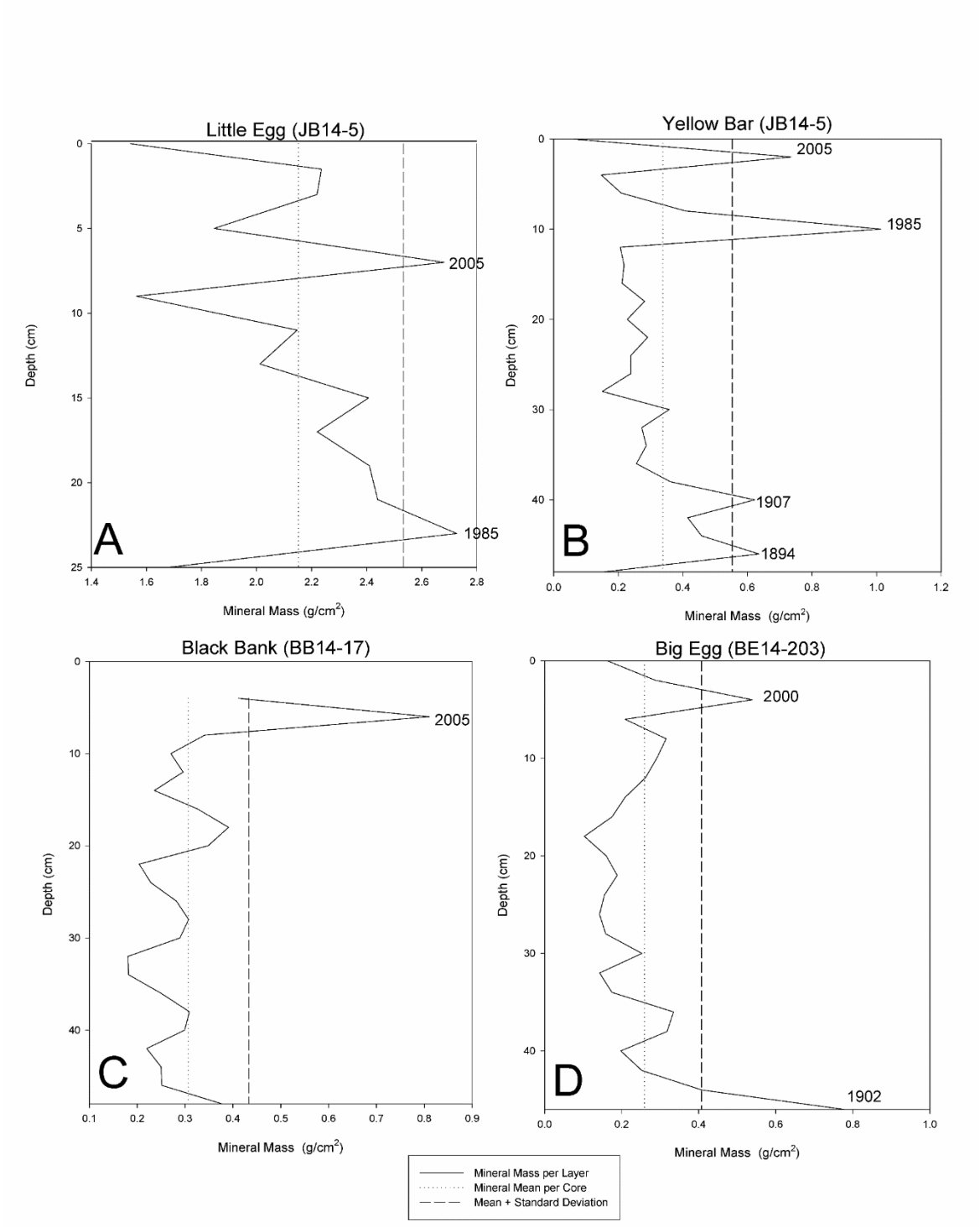

Figure 7. Mineral mass per layer, Mean Mineral Mass per layer, Standard Deviation Mineral Mass per layer + Mean vs. Depth (Average SAR rates used). Cores Shown: Little Egg (a), Yellow Bar (b), Black Bank (c), and Big Egg (d)

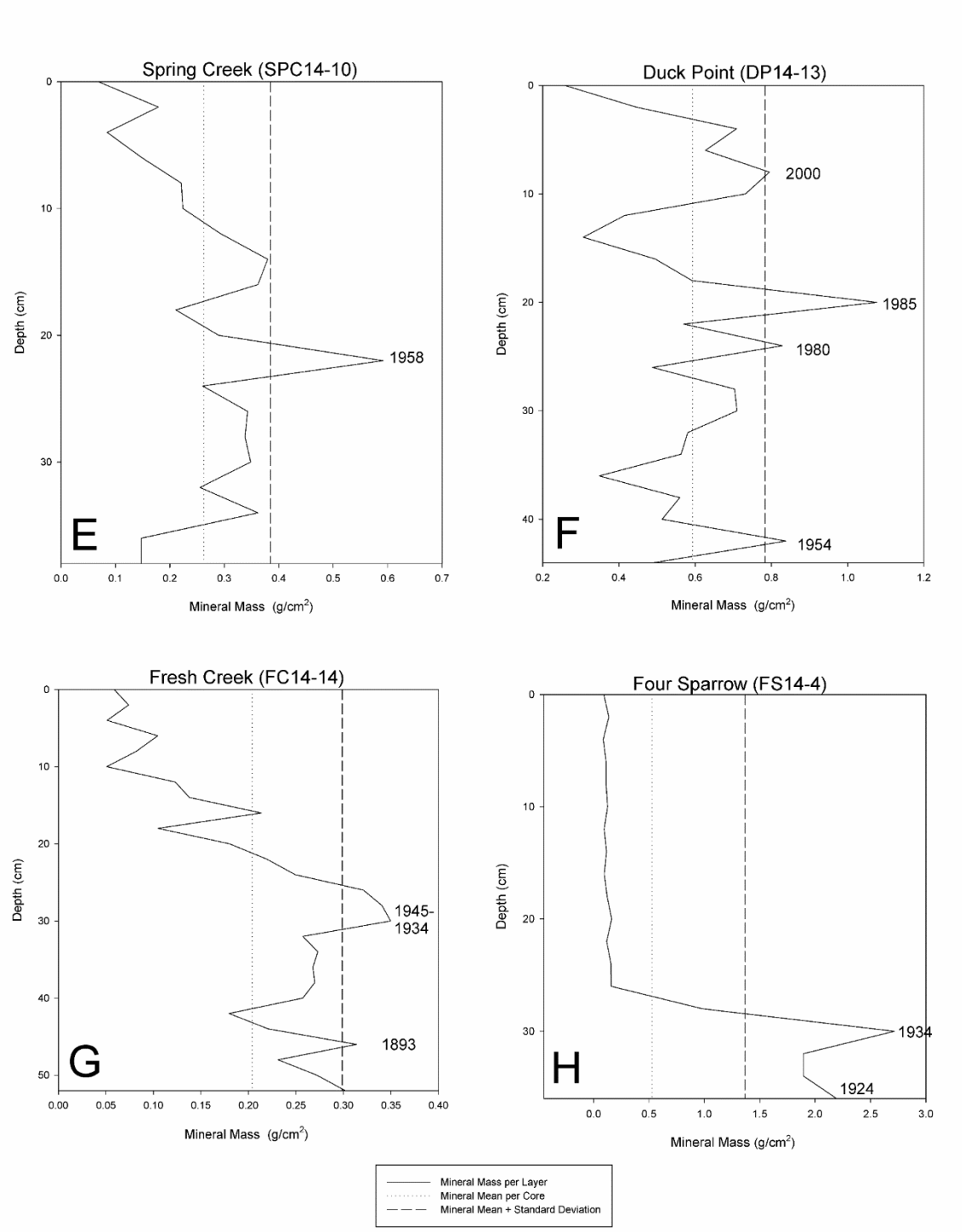

Figure 7 (cont.) Mineral mass per layer, Mean Mineral Mass per layer, Standard Deviation Mineral Mass per layer + Mean vs. Depth (Average SAR rates used). Cores Shown: Spring Creek (e), Duck Point (f), Fresh Creek (g), and Four Sparrow (h)

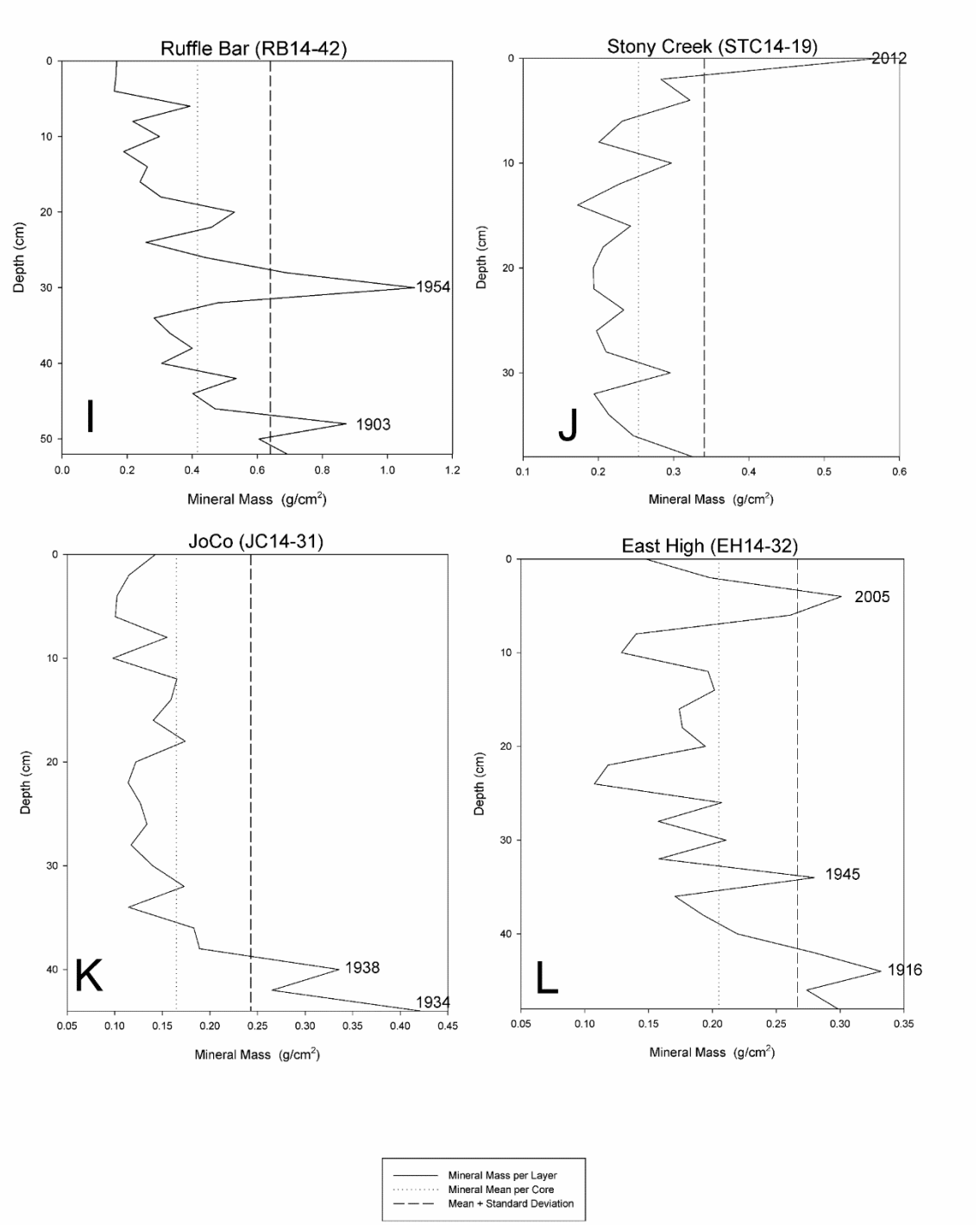

Figure 7 (cont.) Mineral mass per layer, Mean Mineral Mass per layer, Standard Deviation Mineral Mass per layer + Mean vs. Depth (Average SAR rates used). Cores Shown: Ruffle Bar (i), Stony Creek (j), JoCo (k), and East High (l)

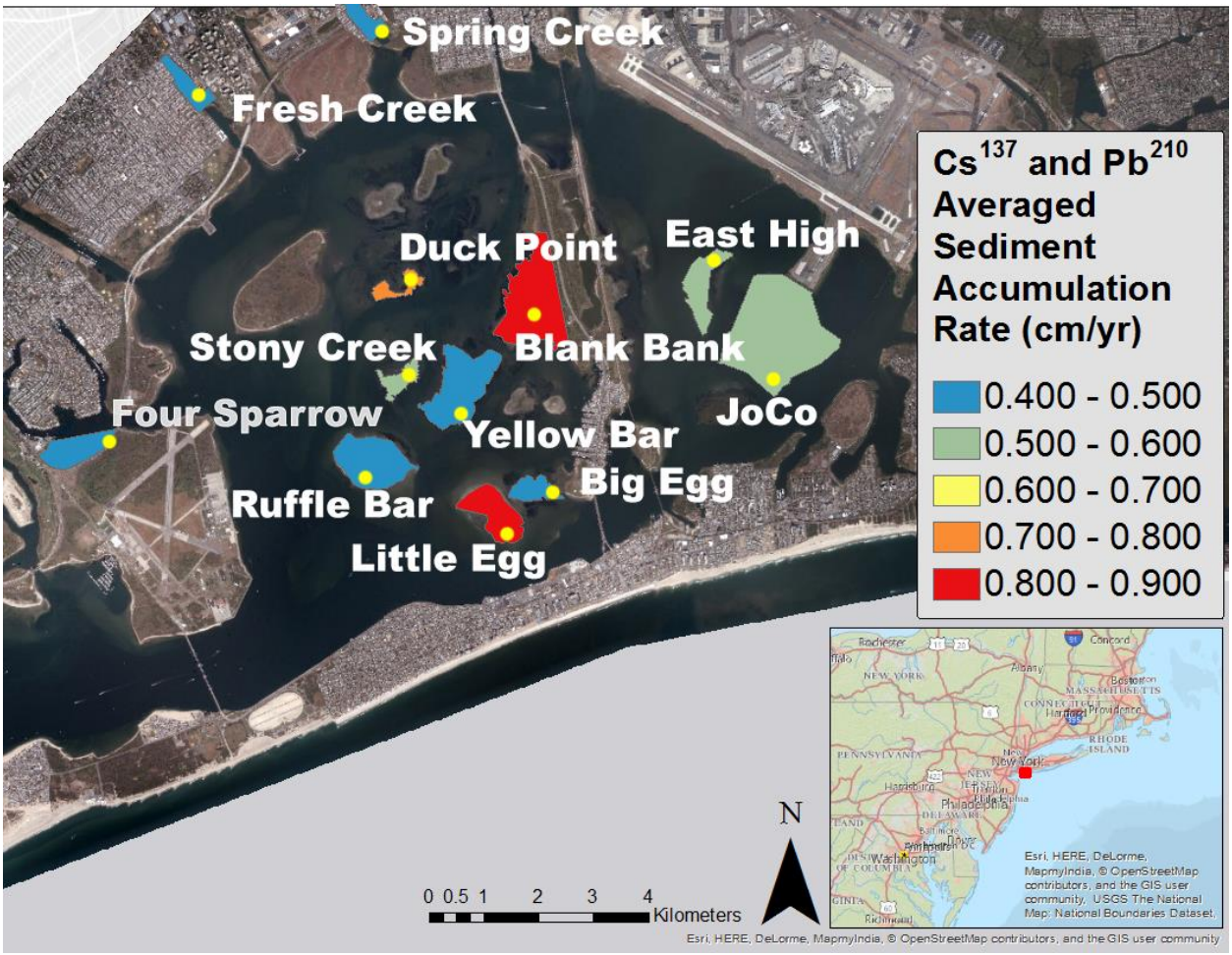

Figure 8. Cs^{137} and Pb^{210} Averaged sediment accumulation rate ($cm\text{-}yr^{-1}$). (Note: erosion was not considered and spatial variation of deposition was not considered due to the limitation of cores collected)

Table 4.1. Event layers from each core correlated to storms within 200km of coring location site from 1954 to 2013 (mineral accumulation is in g/cm^2 (Average SAR from all four methods used). Intensity shown by year is intensity at Long Island landfall. (ET = extra-tropical storm, TS = tropical storm, TD = tropical depression, H1-H5 = category 1 to category 5 hurricanes)

Core Sites	Number of Layers detected in Core	Andrea 2013 (ET)	Sandy 2012 (ET)	Irene 2011 (TS)	Twenty Two 2005 (ET)	Cindy 2005 (ET)	Charley 2004 (ET)	Gordon 2000 (ET)	Gloria 1985 (H1)	Carol 1954 (H3)
East High	4					0.30				
JoCo	2									
Blank Bank	1				0.81					
Big Egg	3							0.54		
Little Egg	2				2.68				2.73	
Four Sparrow	2									
Duck Point	3							.79	1.08	0.84
Yellow Bar	3				.74				1.01	
Spring Creek	1		0.67							
Fresh Creek	5									
Stony Creek	1									
Ruffle Bar	2									0.69
Total Storm Accumulation by Event	28		1.26			4.58		1.33	4.82	1.53

Table 4.2. Event layers from each cores correlated to storms within 200km of coring location site from 1877 to 1945 (mineral accumulation is in g/cm^2 (Average SAR from all four methods used). Intensity shown by year is intensity at Long Island landfall (ET = extra-tropical storm, TS = tropical storm, TD = tropical depression, H1-H5 = category 1 to category 5 hurricanes)

Core Sites	**1945 (TD)**	**Two 1944 storms (ET/H1)**	**1938 (H3)**	**1934 (TS)**	**1924 (TS)**	**1916 (ET)**	**1915 (ET)**	**1904 (ET)**	**1903 (H1)**	**1902 (ET)**	**1900 (ET)**	**1899 (ET)**	**1894 (H1)**	**1893 (H1)**	**1879 (H1)**	**1877 (ET)**	**Total Storm ML by Location (g/cm^2)**	**Percent of Event ML found within core**
East High	0.28				0.33	0.57											1.48	11.7%
JoCo			0.37	0.27													0.60	18.1%
Blank Bank																	0.81	11.5%
Big Egg								0.41			0.78						1.73	8.7%
Little Egg																	5.41	17.9%
Four Sparrow				2.71	2.19												4.91	40.6%
Duck Point																	2.62	25.9%
Yellow Bar													0.64				2.38	35.5%
Spring Creek																	0.67	1.3%
Fresh Creek	0.32		0.34	0.35									0.31		0.30		1.63	12.1%
Stony Creek																	0.57	11.3%
Ruffle Bar								0.69									1.38	17.4%
Total Storm accumulation by Event	0.60		0.68	1.36	2.53	0.57		1.10			0.78		0.95		0.30		22.39	19.8%

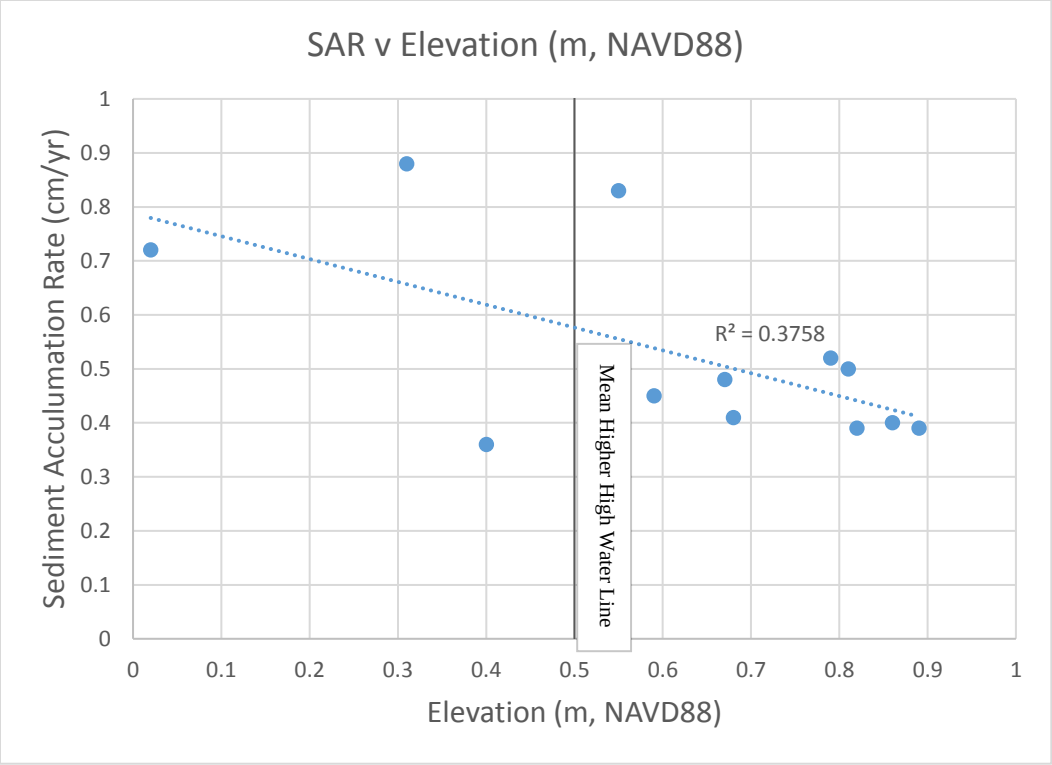

Figure 9. Elevation of all core sites versus Averaged SAR Accumulation Rates

DISCUSSION

In Smith et al.'s (2015) work in Breton Sound, Louisiana, documented storm deposition across the study area is seen widely distributed throughout most cores, whereas our data show no storm events represented in more than three cores. This could be the result of conditions similar to those modeled by Hu et al. (2017), wherein local geomorphology exerts strong control on the local depositional processes. In contrast, the Smith et al. (2015) study area is relatively wide, planar, and more uniform geomorphically. Apart of geological differences, Smith et al. were documented major hurricanes of Category 3 and above whereas the criteria in this study encapsulates all systems within a larger radius. Smith et al. (2015) looked at what role hurricanes play in sediment delivery to the subsiding Mississippi River delta. Like this study, Smith et al. (2015) analyzed multiple cores using ^{210}Pb and ^{137}Cs to compare with mineral peaks within the core to correlate historical storm events with those peaks. They found these storm events only account for 13% of total sediment accumulation and an average sediment accumulation rate of 0.76 cm-yr^{-1} across 27 cores (Smith et. al, 2015).

Wetland SARs commonly exhibit positive correlation with sediment elevation with respect to tidal inundation (Hu et al., 2018, Wang et al., 2017, Smith et al., 2015) In order to evaluate effects of elevation on SAR, Averaged SAR results were compared to the sediment surface elevation for each core location, derived from LIDAR (Wang et al., 2017), in Figure 9. A linear correlation of sediment elevation versus SAR showed an R^2 value of 0.38, indicating that most variation of SARs cannot be explained by low-marsh/high marsh elevation relation with sediment accumulation and other factors such as distance from Rockaway inlet or from the channels are also in play (e.g., Wang et al., 2017; Hu et al., 2018).

Total mineral sediment accumulation in the study area is 112.9 g/cm^2 over the average age span of 90.36 years for all cores. 22.4 g/cm^2 or 19.8% of this amount is identified as mineral accumulation brought about by storm events. Within these anthropogenically altered wetlands, dredging, ditching and landfills could account for some of these apparent event layers. Because of these variables, it is possible some of these event layers are the result of human activities, not storm sedimentation.

Little Egg has the largest amount of mineral content within its core than any of the other ones (Table 4.2). This can be due to geographic, tidal, and/or anthropogenic influence (Hartig et al., 2002). Considering its site location is one of the closest to the opening of Rockaway Inlet (Figure 8), it would seem understandable that the initial surge of many of the storms that pass through deposit a relatively higher amount on the marshes closer to the entry path of the surge (Wang et al., 2017). Generally, the eastern side of the marsh is relatively healthier than the western portion. This is most noted in the contrast between JoCo Island to the east and Yellow Bar to the West (Hu et al., 2017). Hartig et al. (2002) treats Yellow Bar as the main example of pre and post urbanization for Jamaica Bay. Post urbanization in Jamaica Bay is documented as narrow bands of vegetation adjacent to filled land on one side with the open bay on the other. (USDA, 2001). Three extra-tropical storms that all made landfall within the window uncertainty for one mineral peak (Hurricane Charley in 2004, "Twenty-Two" in 2005, and Hurricane Cindy in 2005), Hurricane Gloria in 1985, and an unnamed hurricane in 1915 are the most prevalent events correlated between many the cores (Table 3).

Another possibility for some larger sediment event layers can be the production of fine-grain sediments from ponding (Adamowicz et al., 2005). Ponding results from the death of wetland vegetation, producing fine grained inorganic sedimentation organics in a salt pool

(DeLaune et al., 1994). Ponding has been observed within marsh interiors throughout Jamaica Bay (Hartig et al., 2002). This sediment is a distinct water saturated dark-gray inorganic sediment that differs from the brown peaty organics deposited through marsh vertical accretion and is also a deeper grey than a tidal induced inorganic mineral deposit (Wilson et al., 2010). This depositional result from ponding can alter results if close attention is not given as these deposits can get mislabeled as a mineral layer (Cahoon et al., 1995).

The lack of a multi-core signal of Sandy is interesting (Table 4), with the observed wind of 120 km/h, waves, and a maximum surge reaching 3.5 m in Jamaica Bay (Wang et al., 2017), one would initially expect an ubiquitous event horizon in terms of mineral deposition across all sites. This is not the case, as seen in Hu et al. (2018) models, study showing general erosion and little sedimentation taking place on both low and high marsh. Erosion during Sandy took place on the western portion of the bay with the largest bed shear stress, i.e. resuspension, was in the Rockaway Inlet (Hu et. al., 2018). Hu et al. 2018 modeled a Hurricane Sandy event to observe any Sandy-induced maximum suspended mud and sand concentrations. The modeled peak values in the Jamaica Bay reached 1.8 km/m^3 and 10 kg/m^3 for mud and sand, respectively. Suspended sand concentrations were found predominately in the western part of the bay and more suspended mud concentrations found on the eastern part of the bay. Considering bed shear stress and more wave action found in the western portion of the bay, the suspended sediment concentrations align appropriately. Large sediment transport during Hurricane Sandy was associated with large relative wave height; this took place dominantly near the Rockaway Inlet (Wang et al., 2017).

CONCLUSIONS

This study provides insight on the geochronology of the Jamaica Bay wetlands, in particular the signals of storm generated event layers in the last 130 years. Analysis of sediment cores from most islands in the wetland provided wider approach to the study of understanding accretion and geochronology. The significant findings can be summarized as follows:

1. The average sediment accumulation rate from all methods (1963 and 1953 ^{137}Cs, CIC and CRS ^{210}Pb methods, is 0.48 centimeters per year with sedimentation rates found highest at Little Egg.
2. Storm sedimentation is important for wetland sustainability but does not provide enough accretion to successfully counteract again relative sea level in the area.
3. Extra-tropical storms have been found to be most important and dominant in storm deposited mineral layers in Jamaica Bay.

Hurricane Sandy was not identified in most cores and generally does not play a large role in mineral accretion for Jamaica Bay in its deposition window

REFERENCES

Adamowicz, S.C. and C.T. Roman. 2005. New England Salt Marsh Pools: A Quantitative Analysis of Geomorphic and Geographic Features. *Wetlands*, 25, pp. 279-288.

Allen, J.R.L. (1990) Salt-marsh growth and stratification: a numerical model with special reference to the Severn estuary, southwest Britain. *Marine Geology*, 95(2):77-96.

Antonioli, F., Anzidei, M., Amorosi, A., Lo Presti, V., Mastronuzzi G., Deiana G., De Falco G., Fontana, A., Fontolan, G., Lisco, S., Marsico A., Moretti, M., Orru, P.E., Sannino, G.M., Serpelloni, E., Vecchio, A. 2017. Sea Level rise and potential drowing of the Italian coastal plains: Flooding risk scenarios for 2100. *Quaternary Science Reviews*. 158; 29-43.

Appleby, P. G. 2001. Chronostratigraphic techniques in recent sediments. In Tracking environmental change using lake sediments, basin analysis, coring, and chronological techniques, development in paleoenvironmental research, ed. W.L. Last and J.P. Smol.

Appleby, P. G., and F. Oldfield. 1978. The calculation of lead-210 dates assuming a constant rate of supply of unsupported 210Pb to the sediment. Catena 5: 1-8.

Appleby, P. G., and F. Oldfield. 1983. The assessment of ^{210}Pb data from sites with varying sediment accumulation rates. *Hydrobiologia* 103: 29-35.

Bentley, S.J., Keen T.R., Blain C.A., W.C. Vaugan 2002. The Origin and Preservation of a Major Hurricane Event Bed in the Northern Gulf of Mexico: Hurricane Camille, 1969. *Marine*

Binford, M. W. 1993. Interpretation of 210Pb profiles and verification of the CRS dating model in PIRLA project lake sediment cores. *Journal of Paleolimnology* 9: 275-296.

Blanco, J.F., E.A. Estrada, L.F. Ortiz, and L.E. Urrego. 2012. Ecosystem-Wide Impacts of Deforestation in Mangrove: The Urabá Gulf (Colombian Carribbean) Cast Study, *International Scholarly Research Network Ecology*, 2012:14.

Bloom, A.L., Stuiver, M. 1963. Submergence of the Connecticut Coast. *Science* (New York, N.Y.). 139:332-4.

Blum, M. and Roberts, H.H. 2009. Drowning of the Mississippi Delta due to insufficient sediment supply and global sea-level rise. *Nature Geoscience*. 2; 488-491.

Boustead B.M, S.D. Hilberg, M.D. Shulski, K.G. Hubbard. 2015. The Accumulated Season Severity Index. *Journal of Applied Meteorology and Climatology*, 54: 1693-1712

Brandon C.M., Woodruff J.D, Donnelly J.P., Sullivan R.M. 2014. How Unique was Hurricane Sandy? Sedimentary Reconstructions of Extreme Flooding from New York Harbor. *Scientific Reports*. 4; 7366.

Bridges, T.S., Wagner, P.W., Burks-Copes, K.A., Bates, M.E., Collier, Z.A.; Fischenich, C.J.; Gailani, J.Z., Leuck, L.D., Piercy, C.D., Rosati, J.D. 2015. Use of Natural and Nature-Based Features (NNBF) for Coastal Resilience; Engineer Research and Development Center.

Cahoon, D.R., Marin P.E., Black B.K., J.C. Lynch. 2000. A method for measuring vertical accretion, elevation, and compaction of soft, shallow-water sediments. *Journal of Sedimentary Research,* 70(5):1250-1253.

Cahoon D.R., Reed D.J, Day J.W. 1995. Estimating shallow subsidence in microtidal salt marshes of the southeastern United States: Kaye and Barghoorn revisited. *Marine Geology*. 128:1-9.

Chmura G.L. and Hung G.A. 2004. Controls on salt marsh accretion: A test in salt marshes of Eastern Canada. *Estuaries and Coasts.* 27; 70-81.

Church, J.A., N.J. White. 2006. A 20th Century Acceleration in Global Sea-Level Rise. *Geophysical Research Letters*, 33, L01602.

City of New York Local Law 71. 2005.

City of New York. A Stronger, More Resilient New York. New York, NY, 2013; 445.

Cochran, J.K., P. Masqué. 2003. Short-lived U/Th series radionuclides in the ocean: tracers for scavenging rates, export fluxes and particle dynamics. *Reviews in Mineralogy and Geochemistry,* 52:461–492. *Continental Shelf Research*, 20:1621-1634

Corcoran M. & Kelley J. 2006. Sediment Tracing technology: An Overview. ERCD TN SWWRP 06-10

Cunha, I.I.L. 2001. ^{210}Pb and ^{137}Cs geochronologies in the Cananeia-Iguape Estuary (São Paulo, Brazil). *Journal of Radioanalytical and Nuclear Chemistry*. 249; 257-261.

Cutshall, N.H., Larsen, I.L., Olsen C.R., 1983. Direct Analysis of 210Pb in Sediment Samples: Self Absorption Corrections. *Nuclear Instruments and Methods in Physics Research,* 206(1):309-312.

DeLaune, R. D., J. A. Nyman, and W. H. Patrick, Jr. 1994. Peat collapse, ponding and wetland loss in a rapidly submerging coastal marsh. *Journal of Coastal Research* 10:1021–1030.

DeLaune, R. D., Jugsujinda, A., Peterson, G. W. and W.H. Patrick 2003. Impact of Mississippi River freshwater reintroduction on enhancing marsh accretionary processes in a Louisiana estuary. *Estuarine, Coastal, and Shelf Science*, 58(3): 653–662.

Delaune, R., Baumann, R., Gosselink J. 1983. Relationships Among Vertical Accretion, Coastal Submergence, and Erosion in a Louisiana Gulf Coast Marsh. *Journal of Sedimentary Petrology,* 53:147-157.

Denommee, K.C., S.J. Bentley, A.W. Droxler. 2014. Climatic Controls on Hurricane Patterns: a 1200-y Near Annual Records from Lighthouse Reef, Belize. *Scientific Reports*. 4 Dordrecht: Kluwer Academic Publishers.

Enos, S. 2015. Reconstruction of the Post-Glacial Formation of the Peddocks Island Salt Marsh, Hull, MA. *Standard Theses*. Paper 23.

Fagherazzi, S. 2013. The ephemeral life of a salt marsh. *Geology.* 41.8:943-944.

Fagherazzi, S. 2012. Numerical models of salt marsh evolution: Ecological, geomorphic, and climatic factors, *Reviews of Geophyics*. 50:RG1002.

French, J. 2006. Tidal marsh sedimentation and resilience to environmental change: exploratory modeling of tidal, sea level and sediment supply forcing in predominately allochthonoussystems (2006). *Marine Geology,* 235:119-136. *Geology,* 186:423-446.

Gornitz ,V., Couch S, Hartig E. 2001. Impacts of sea level rise in the New York City metropolitan area. *Global and Planetary Change,* 32:61-88.

Gornitz, V. 1995. Sea-level rise: A review of recent past and near-future trends. *Earth Surface Processes and Landforms*, 20:7-20.

Hanson, H., Brampton, A., Capobianco, M., Dette, H., Hamm, L., Laustrup, C., Lechuga, A., Spanhoff, R. Beach. 2002. Nourishment projects, practices, and objectives—A European overview. *Coastal Engineering,* 47:81–111.

Hartig, E.K., Gornitz, V., A. Kolker, et al. 2002. Anthropogenic and climate-change impacts on salt marshes of Jamaica Bay, New York City. *Wetlands*, 22:71.

Heiri O., Lotter A.F., G. Lemcke. 2001. Loss on ignition as a method for estimating organic and carbonate content in sediments: reproducibility and comparability of results. *Journal of Paleolimnology,* 25:101–110.

Holland, G.J. 2012. Hurricanes and rising global temperatures. *Proceedings of the National Academy of Sciences of the United States of America,* 109(48):19513-19514.

Hu, K., Chen, Q., Wang, H., Hartig, E.K. and Orton, P.M., 2018. Numerical modeling of salt marsh morphological change induced by Hurricane Sandy. *Coastal Engineering*, *132*, pp.63-81.

Irish, J.L., D.T. Resio, J.J. Ratcliff. 2008. The Influence of Storm Size on Hurricane Surge. . Journal of Applied Meteorology and Climatology, 38: 2003-2013

Hanafin J.A.,, Y. Quilfen, F. Ardhuin, J. Sienkiewicz, P. Queffeulou, M. Obrebski, B. Chapron, N. Reul, F. Collard, D. Corman, E.B. De Azevedo, D. Vandemark, E. Stutzmann. 2012. Phenomenal Sea States and Swell from a North Atlantic Storm in February 2011: A Comprehensive Analysis. 2012. *American Meterological Society;* 93. 1825-1832

Jones, S.C., Harr, P.A., Abraham, J., Bosart, L.F., Bowyer, P.J., Evans, J.L., Hanley, D.E., Hanstrum, B.N., Hart, R.E., Lalaurette, F., Sinclair, M.R., Smith, R.K., Thorncroft, C. 2003: The Extratropical Transition of Tropical Cyclones: Forecast Challenges, Current Understanding, and Future Directions. Weather and Forecasting, 18, 1052-1092.

Karvetski, C., R.B. Lund, & F. Parisi. 2009. A statistical study of extreme nor'easter snowstorms. Involve 2: 341–350.

Kearney, M.S. and Turner, R.E., 2016. Microtidal marshes: Can these widespread and fragile marshes survive increasing climate–sea level variability and human action?

Kendall C. St. C. 1981. Carbonates and relative changes in sea level. *Marine Geology*. 44;181-212.

Knutson, T.R., Mcbride, J.L., Chan, J., Emanuel, K., Holland G., Landsea C., Held, I., Kossin J.P., Srivast A., M. Sugi. 2010. Tropical cyclones and climate change. *Nature Geosciences,* 3:157-163 extra

Kolker, A.S. 2005. The impacts of climate variability and anthropogenic activities on salt marsh accretion and loss on Long Island. Ph.D. thesis, Stony Brook University, Stony Brook.

Letzch, W.S., R.W. Frey. 1980. Deposition and erosion in a Holocene salt marsh, Sapelo Island, Georgia. *Journal of Sedimentary Research* 50(2):529-542.

Merguerian, C., Sanders J.E., Trips on the Rocks – Guide 13: Glacial Geology of Long Island,

Morris, J.T., Barber, D.C., Callaway J.C., Chambers, R., Hagen, S.C., Hopknison C.S., Johnson, B.J., Megonigal P., Neubauer S.C., Troxler T., Wigand, C. 2016. Contributions of organic and inorganic matter to sediment volume and accretion in tidal wetlands at steady state. *Earth's Future (AGU).* 4; 110-121.

Morris, J.T., P.V. Sundareshwar, C.T. Nietch, B. Kjerfve, D.R. Cahoon. 2002. Responses of Coastal Wetland to Rising Sea Level. *Ecological Society of America* 83; 2869-2877.

Mudd, S.M. 2011. The life and death of salt marshes in response to anthropogenic disturbance of sediment supply. *Geology*, 39(5):511-512

Muhammad, Z., Bentley, S.J., Febo, L.A., Droxler, A.W., Dickens, G. R., Peterson, L.C., B.N. Opdyke 2008. Excess ^{210}Pb inventories and fluxes along the continental slope and basins of the Gulf of Papua: *Journal of Geophysical Research: Earth Surface (2003– 2012*). 113:F1.

National Parks Service (NPS). 2007. An Update on the Disappearing Salt Marshes of Jamaica Bay, New York. Jamaica Bay Watershed Protection Plan Advisory Committee.
New York. (2010) Duke Geological Laboratory, 2010. PDF.

Nittrouer J.A., E. Viparelli. 2014. Sand as a stable and sustainable resource for nourishing the Mississippi River delta. *Nature Geoscience 7, 350-354*

Nittrouer, C., R. Sternberg. 1981. The formation of sedimentary strata in an allochthonous shelf environment: the Washington continental shelf. *Marine Geology* 42:201–232.

Nittrouer, C.A., Demaster, D.J., B.A., Cutshall, N.H., Larsen,I.L., (1983/1984), The Effect of Sediment Mixing on a Pb-210 Accumilation Rates for the Washington Continental shelf. *Marine Geology*, 54: 201-221.

Noller, J. S. 2000. Lead-210 geochronology: Quaternary Geochronology: Methods and applications. Washington, DC: American Geophysical Union.

NYC, Nyc hazards nyc hurricane history, New York City Office of Emergency Management 2013c.

NYC-DEP. 2007. Jamaica Bay Watershed Protection Plan; New York City Department of Environmental Protection (DEP): New York, NY, USA, 1:128.

NYC-DEP. 2014. Jamaica Bay Watershed Protection Plan; New York City Department of Environmental Protection (DEP): New York, NY, USA, 1:56.

Nyman, J.A., Walters R.J., Delaune R.D., Patrick W.H. 2006. Marsh Vertical Accretion via Vegetative Growth. Estuarine, *Coastal and Shelf Science*. 69.3-4:370-380.

Orson R.A., Stevenson J.C. 2008. Site-Specific Scenarios for Wetlands Accretion as Sea Level Rises in the Mid-Atlantic Region. *Background Documents Supporting Climate Change Science Program Synthesis and Assessment Product 4.1:2.1.*

Orton, P., Talke S., et al. 2015. Channel Shallowing as Mitigation of Coastal Flooding. *Journal. Marine Science and Engineering*, 3:654-673.

Orton, P., Vinogradov, S., Georgas, N., Blumberg, A., Lin, N., Gornitz, V., Little, C., Jacob, K., R. Horton. 2015. New York City Panel on Climate Change 2015 Report Chapter 4: Dynamic Coastal Flood Modeling. *Ann. N. Y. Acad. Sci.* 1336:56–66.

Pejrup, M., T.J Anderson. 2000. The influence of ice flow on sediment transport, deposition and reworking in a temperate intertidal mudflat area, the Danish Wadden Sea.

Pendleton, L. 2008. The Economic and Market Value of Coasts and Estuaries: What's at Stake? Restore America's Estuaries, Arlington, VA. 182.

R.S. Lewis and J.R. Stone. 1991. Late Quaternary stratigraphy and depositional history of the Long Island Sound basin: Connecticut and New York. *Journal of Coastal Research.*; 11. 1-23.

Redfield, A. C. 1972. Development of a New England Salt Marsh. *Ecological Monographs*, 42:201–237.

Redfield, A.C. 1967. Postglacial Change in Sea Level in the Western North Atlantic Ocean. *Science*. 157(3789):687-692

Reed, D. J. 1990. The impact of sea-level rise on coastal salt marshes. Progressing Physical Geography 14:465-481.

Reed, D.J., Bishara D.A., Cahoon D.R., Donnelly J., Kearney M., Kolker A.S., Leonard L.L, S.M. Mudd, A. D'Alpaos, J.T. Morris. 2010. How does vegetation affect sedimentation on tidal marshes? Investigating particle capture and hydrodynamic controls on biologically mediated sedimentation. *Journal of Geophysical Research*; 115.

Sharma, S., Kumar V.S., R. Gowthaman. 2017. Textural characteristics and morphosedimentary environment of foreshore zone along Ganpatipule, Maharashtra, India. *Marine Georesources & Geotechnology*. 35(6):1-8.

Siverd, C. 2013. Jamaica Bay: Flood Fish Reduction System Conceptual Final Report. TU Delft.

Smith, J. E. et al. 2015. What Role do Hurricanes Play in Sediment Delivery to Subsiding River Deltas? *Scientific Reports*, *5*:17582.

Stumpf, R.P. 1983. The Process of sedimentation in the surface of a salt marsh. *Estuarine Coastal Shelf Sciences* 17:495-508.

Swanson, R., West-Valle, A., C. Decker. 1992. Recreation vs. waste disposal: The use and management of Jamaica Bay. *Long Island History. J.*, 5:21–41.

Swanson, R.L., R.E. Wilson. 2008. Increased tidal ranges coinciding with Jamaica Bay development contribute to marsh flooding. *Journal of Coastal Research*. 24(6)1565–1569.

Tanski J. 2007. , Long Island's Dynamic South Shore: A Primer on the Forces and Trends Shaping Our Coast

Uchupi E., N. Driscoll, R.D. Ballard, S.T. Bolmer. 2001. Drainage of late Wisconsin glacial lakes and the morphology and late quarternary stratigraphy of the New jersey- southern New England continental shelf and slope. Marine Geology, 172; 117-145

Vail, P.R., Mitchum., R.M., Thompson S. 1977. Seismic Stratigraphy and Global Change of Sea Level: Part 3. Relative Changes of Sea Level from Coastal Onlap: Section 2. Application of Seismic Reflection Configuration to Stratigrapic Interpretation. *Seismic Stratigraphy*. 26; 63-81.

Van Sickel, W. A., Kominz, M. A., Miller, K. G. and Browning, J. V. 2004, Late Cretaceous and Cenozoic sea-level estimates: backstripping analysis of borehole data, onshore New Jersey. Basin Research, 16: 451–465.

Wang, H., Chen, Q., Hu, K., Snedden, G.A., Hartig, E.K., Couvillion, B.R., Johnson, C.L. and Orton, P.M., 2017. *Numerical modeling of the effects of Hurricane Sandy and potential future hurricanes on spatial patterns of salt marsh morphology in Jamaica Bay, New York City* (No. 2017-1016). US Geological Survey.

Webster P.J., G.J. Holland, J.A. Curry, H.-R. Chang. 2005. Changes in tropical cyclone number, duration, and intensity in a warming environment. *Science*, 309:1844-1846

Wilson C.A., M.A. Allison. 2008. An equilibrium profile model for retreating marsh shorelines in southeast Louisiana. *Estuarine Coast Shelf Science*, 80:483–494.

Wilson, K.R., J.T. Kelley, A. Croitoru, M. Dionne, D.F.Delknap, R. Steneck, 2009. Stratigraphic and Ecophysical Characterizations of Salt Pools: Dynamic Landforms of the Webhannet Salt Marsh, Wells, ME, USA. *Estuaries and Coasts*, pp. 855-870.

Wilson, K.R., J.T. Kelley, B.R. Tanner, D.F. Belknap, 2010. Probing the Origins and Stratigraphic Signature of Salt Pools from North-Temperate Marshes in Maine, USA. *Journal of Coastal Research*, pp. 1007-1026.

Wolters M, Bakker J.P., Bertness MD, Jefferies RL, Moller I. 2005. Saltmarsh erosion and restoration in south-east England: squeezing the evidence requires realignment. *J. Appl. Ecol.* 42:844–51.

VITA

Ryan Clarke, a native of Baton Rouge, Louisiana, received his Bachelor's Degree in Science at Louisiana State University (LSU). He has mentored high school students at LSU and has worked hard to promote the beauty of Science to his mentees. He was accepted in the Geology and Geophysics Master's Program under Dr. Samuel Bentley majoring in coastal sedimentology. He anticipates graduating with his M.S. degree in May 2018. He plans to continue his Earth Science path for many years to come.